Quantifying tropical cyclone's effect on the biogeochemical processes using profiling float observations in the Bay of Bengal

M. S. Girishkumar[1], V. P. Thangaprakash[1*], T. V. S. Udaya Bhaskar[1], K. Suprit[1], N. Sureshkumar[1], S. K. Baliar Singh[1], J. Jofia[1], V. Pant[2], S. Vishnu [1], G. George[3], K. R. Abhilash[4], S. Shivaprasad[1]

[1]Indian National Centre for Ocean Information Services (INCOIS), Hyderbad-500090, India.

[2]Centre for Atmospheric Sciences, Indian Institute of Technology Delhi, New Delhi, India.

[3]Central Marine Fisheries Research Institute (CMFRI), Kochi-682018, Kerala, India.

[4]National Centre for Sustainable Coastal Management (NCSCM), Chennai- 600025, Tamil Nadu, India.

*_Corresponding author address_: V. P. Thangaprakash, Indian National Centre for Ocean Information Services (INCOIS), Hyderbad-500090, INDIA, Email: thangaprakash.vp@incois.gov.in. Phone: +91-40-23886168, Fax: +91-40-23892910.

This article has been accepted for publication and undergone full peer review but has not been through the copyediting, typesetting, pagination and proofreading process which may lead to differences between this version and the Version of Record. Please cite this article as doi: 10.1029/2017JC013629

Abstract

Physical and biogeochemical observations from an autonomous profiling Argo float in the Bay of Bengal show significant changes in upper ocean structure during the passage of Tropical Cyclone (TC) *Hudhud* (7–14 October 2014). TC *Hudhud* mixed water from a depth of about 50 m into the surface layers through a combination of upwelling and turbulent mixing. Mixing was extended into the depth of nutricline, the oxycline and the subsurface-chlorophyll-maximum; thus had a strong impact on the biogeochemistry of the upper ocean. Before the storm, the near-surface layer was nutrient depleted and was thus oligotrophic with the chlorophyll-*a* concentration of less than 0.15 mg m^{-3}. Storm mixing initially increased the chlorophyll by 1.4 mg m^{-3}, increased the surface nitrate concentration to about 6.6 µM kg^{-1}, and decreased the sub-surface dissolved oxygen (30–35 m) to 31 % of saturation (140 µM). These conditions were favorable for phytoplankton growth resulting in an estimated increase in primary productivity averaging 1.5 g C m^{-2} day^{-1} over 15 days. During this bloom, chlorophyll-*a* increased by 3.6 mg m^{-3}, and dissolved oxygen increased from 111 % to 123 % of saturation. Similar observations during TC *Vardah* (6–12 December 2016) showed much less mixing. Our analysis suggests that relatively small (high) translation speed and presence of cold (warm) core eddy leads to strong (weak) oceanic response during TC *Hudhud* (TC *Vardah*). Thus, although cyclones can cause strong biogeochemical responses in the Bay of Bengal, the strength of response depends on the properties of the storm and the prevailing upper ocean structure such as presence of mesoscale eddies.

1. Introduction

The Bay of Bengal (BoB) is an active region for the formation of Tropical Cyclones (TCs), one of the most devastating natural disasters in the world. Annually, on an average 3–4 TCs (about 5 % of the global TCs) forms in the BoB [*Alam et al.* 2003]. TC's occurs more frequently during October–December (primary TC peak season) and May–June (secondary TC peak season) in the BoB. The presence of favourable oceanic and atmospheric conditions leads to the TC development and intensification during these periods [*Li et al.,* 2013; *Girishkumar et al.,* 2015].

The BoB receives large amounts of freshwater from river discharge and seasonal monsoon rainfall [*Varkey et al.,* 1996, *Prasad*, 1997; *Rao and Sivakumar*, 2003]. The copious freshwater flux into the BoB makes the waters in the near-surface layer less saline compared to subsurface layers, leading to persistent occurrence of strong halocline in the near-surface layer throughout the year [*Shetye et al.*, 1996; *Thadathil et al.*, 2007; *Girishkumar et al.,* 2011; *Girishkumar et al.,* 2013a; *Mahadevan et al.,* 2016]. The main consequence of presence of salt stratification in the near surface layer in the BoB leads to the formation of barrier layer; the layer between base of the mixed layer (MLD) and the isothermal layer (ILD) [*Lukas and Lindstrom*, 1991*; Vinayachandran et al.*, 2002; *Rao and Sivakumar*, 2003; *Thadathil et al.,* 2007; *Girishkumar et al.,* 2011; *Girishkumar et al.,* 2013a; *Thangaprakash et al.,* 2016; *Thadathil et al.,* 2016]. As reported in earlier studies, both barrier layer and near-surface salt stratification can play a significant role in the seasonal evolution of phytoplankton variability in the BoB [*Gomes et al*., 2000; *Kumar et al*., 2002; *Narvekar and Kumar*, 2006; 2014; *Lévy et al.,* 2007*; Gomes et al.,* 2016]. The strong haline stratification inhibits upward flux of nutrient-rich subsurface water into the euphotic zone, which leads to significantly low biological productivity in the BoB, as compared with the Arabian Sea [*Gomes et al*., 2000; *Kumar et al.,* 2002; *Narvekar and Kumar*, 2014]. Another important

factor affecting the biological productivity during the summer monsoon (June–September) in the BoB is the presence of monsoonal-cloud cover which hinders the incoming shortwave radiation [*Gomes,* 2000*; Madhupratap et al.,* 2003; *Madhu et al.,* 2006*; Gomes et al.,* 2016]. Subsequently, large quantities of suspended sediments transported by the rivers draining into the BoB may significantly reduce downward penetration of solar radiation in the water column [*Gomes,* 2000*; Madhupratap et al.,* 2003; *Madhu et al.,* 2006*; Gomes et al.,* 2016]. However, recent observational and modelling studies show that during favorable conditions, there is considerable enhancement of chlorophyll in the near-surface layer at certain regions in the BoB on the seasonal scale [*Vinayachandran and Mathew, 2003; Vinayachadran et al.,* 2004; *Kumar et al., 2004; Vinayachandran et al.,* 2005; *Narvekar and Kumar,* 2006; *Murtugudde et al.,* 1999; Vinayachandran, 2009*; Girishkumar et al.,* 2012; *Currie et al.,* 2013; *Lim et al.,* 2013; *Kumar et al., 2004; Gomes et al., 2016*]. Also, there are notable efforts to document the interannual variability of the chlorophyll in the BoB [*Murtugudde et al.,* 1999; *Vinayachandran and Mathew, 2003; Girishkumar et al.,* 2012; *Martin and Shaji*, 2015; *Gomes et al.,* 2016 and *references therein*]. These studies show that different physical processes (such as, open ocean upwelling, eddies, westward-propagating-upwelling Rossby waves, and vertical mixing due to wind events) erodes the near-surface stratification, which can lead to the enhancement of chlorophyll in the near-surface layer through the upward flux of nutrient-rich subsurface water into the euphotic zone. Enhancement of chlorophyll in the BoB in response to TCs has also been documented in various studies [*Vinayachandran and Mathew,* 2003; *Rao et al.,* 2006; *Smitha et al.,* 2006; *Reddy et al.,* 2008; *Tummala et al.,* 2009; *Maneesha et al., 2011; Chen et al.,* 2013].

Most of these earlier studies are based on satellite measurements of ocean colour, which provides the spatio-temporal evolution of chlorophyll over large oceanic areas. However, ocean colour satellites (primarily visible and infra-red band) are incapable to

observe through clouds and below the ocean surface. Hence, the satellite measurements of chlorophyll during the period of intense TC activities are severely hampered by cloud cover, resulting in the scarcity of observations and understanding during the period of a TC. Ship-based *in situ* observations can provide high-quality information on the subsurface biogeochemical variables, but are not feasible during violent wind and high wave conditions associated with a TC. The importance of the TC forcing on the upper ocean biogeochemical processes is well recognised and linked to the state of the total marine ecosystem [*Naik et al.,* 2008; *Hung et al.,* 2010; *Chung et al.,* 2012; *Fiedler et al.,* 2013; *Yu et al.,* 2013; *Paul et al.,* 2013*; Chang et al.,* 2014]. Hence, a better understanding of the upper ocean biogeochemical response to TC is worth investigating and crucial to the well-being of the economy and fisheries of the region. However, owing to the dearth of systematic and high-quality *in situ* measurements of biogeochemical variables during the cyclonic period, studies quantifying oceanic biogeochemical response to TCs through *in situ* observations are very limited in the BoB. Autonomous profiling floats, such as Biogeochemical Argo (BGC-Argo) floats, equipped with biogeochemical and Conductivity-Temperature-Depth (CTD) sensors are capable of collecting good quality *in situ* subsurface measurements on different temporal scales, particularly during extreme weather conditions such as TC. Hence, biogeochemical and physical data (both surface and subsurface) from these profiling floats provides an unmatched and distinctive advantage to enhance our understanding on the impact of TC's on biogeochemical variability [*Ravichandran et al.,* 2012; *Chacko et al.,* 2017].

A BGC-Argo float (WMO ID 2902114; hereafter C-Float (Chlorophyll-Float)) made observations very close to the TC *Hudhud* track during 7–14 October 2014 and TC *Vardah* track during 6–12 December, 2016 in the central BoB (Figure 1; C-Float locations are mapped as dark-purple (when near to TC) and dark-green colour triangles (entire TC period) during TC *Hudhud* and TC *Vardah* in Figure 1b and Figure 1d respectively). The TC *Hudhud*

and TC *Vardah* life cycles are summarized in the supporting information (S1). The C-Float was equipped with: a Seabird (SBE-41CP) CTD sensor, a Wetlabs AP2 optical backscatter sensor (at a centroid angle of 142° at 700 nm), a chlorophyll fluorescence sensor (excitation wavelength of 470 nm and emission wavelength of 695 nm), and an Aanderaa Optode 4330 sensor to measure dissolved oxygen.

The proximity of the C-Float to the tracks of TC *Hudhud* (13.59 °N and 88.88 °E; ~25 km) and TC *Vardah* (13.97°N and 86.41 °E; ~85 km) provided an unprecedented opportunity to understand the observed variability of upper ocean biogeochemical response to a TC in the BoB. Recently, *Chacko* [2017] have examined only the chlorophyll response to the TC *Hudhud* using the same BGC-Argo float in the BoB. However, in the present study, we extend the analysis independently to include all the biogeochemical variables measured by the C-Float. To make our analysis more robust, we have also adopted and developed improved quality control procedures by utilizing ship-based *in situ* data. These procedures and checks were in addition to the standard BGC-ARGO quality control methods. Moreover, availability of *in situ* observations from the same float during two different TC events also provides a unique opportunity to examine plausible reasons for the differential oceanic response for different TC's. We restrict our analysis to the period between 15 September 2014 to 15 November 2014 for TC *Hudhud* and 15 November 2016 to 15 January 2017 for TC *Vardah*.

Further, the availability of subsurface oxygen data from the C-float ensures that the responses of dissolved oxygen concentrations to the TC were also documented. One of the important characteristics of the BoB is the existence of Oxygen Minimum Zone (OMZ; < 5 µM) in the intermediate depths (100 m – 1000 m), which is weaker than the Arabian Sea OMZ [*Wyrtki et al.*, 1971; *Deuser et al.*, 1975; *Sharma et al.*, 2013; *McCreary et al.*, 2013].

Moreover, no previous studies have documented the impact of TC forcing on the dissolved oxygen concentration in the near-surface layer of the BoB.

The rest of the paper is organized as follows. Section 2 describes datasets used for the study and methodologies followed. Section 3 describes observed upper ocean variability due to TC *Hudhud* and TC *Vardah* forcing and plausible causative factors that modulate the variability. Specifically, following points were addressed in detail:

1. To document the role of TC induced mixing and upwelling along with biogeochemical processes on the observed variability of sub-surface chlorophyll maxima and near surface chlorophyll.
2. To quantify the nutrients enrichment at the near surface layer in response to TC and how the average new production estimated from nitrate flux agrees with the estimation from chlorophyll.
3. To document the role of TC induced mixing and upwelling along with biogeochemical processes on the observed variability of near-surface dissolved oxygen.

In Section 4, a detailed investigation of the role of TC characteristics (such as translation speed and intensity) and pre-existing mesoscale eddy conditions on the observed differential oceanic responses during the TC *Hudhud* and the TC *Vardah* are presented. Results are summarized in Section 5.

2. Data and Methods

Apart from BGC-Argo float data, we have also used various types of *in situ* and satellite data in this study. Daily merged satellite product of chlorophyll-*a* concentration data based on Moderate Resolution Imaging Spectroradiometer (MODIS)-AQUA and Visible and Infrared

Imager / Radiometer Suite (VIIRS) with the spatial resolution of 4 km obtained from GlobColour were used to characterize the surface bloom in this study [*Maritorena et al.,* 2010; *Fanton-d'Andon et. al.,* 2009]. Daily averaged Outgoing Long wave radiation (OLR) data from Advanced Very High Resolution Radiometer (AVHRR) on board KALPANA–I satellite with the spatial resolution of 0.25° is used as a proxy for the atmospheric convection [*Mahakur et al.,* 2013]. The Advanced Scatterometer (ASCAT) ocean surface wind data obtained from Asia Pacific data research Centre [*Bentamy and Fillon,* 2012] with a spatial resolution of 0.25° and TropFlux radiative and turbulent heat flux data [*Praveen Kumar et al.,* 2011] are utilized to assess the impact of net surface heat flux on the observed variability of mixed layer depth. Advanced Microwave Scanning Radiometer for EOS (AMSR-E), AMSR-2, Tropical Rainfall Measuring Mission (TRMM) Microwave Imager (TMI) and WindSAT Microwave Optimum Interpolation Sea Surface Temperature product (MW-OISST) with 0.25° (~25 km) grid spacing [*Gentemann et al.,* 2003] are used to understand spatio-temporal evolution of SST. Merged-gridded Sea level anomaly (SLA) from different altimeter measurements (Jason-3; Sentinel-3A, OSTM/Jason-2 interleaved; SARAL-DP/AltiKa; Cryosat-2) at delayed time from Copernicus Marine Environment Monitoring Services (CMEMS) are used to characterize the signature of mesoscale features in the BoB. Three hourly best TC tracks of both TC *Hudhud* and TC *Vardah* were obtained from Regional Specialised Meteorological Centre (RSMC), India Meteorological Department (IMD), India (http://www.imd.gov.in/section/nhac/dynamic/bestrack.htm) to examine the life cycle of TC.

The C-Float acquires data at pre-determined depths once in every 5 days during ascent and surfaced at 1700 hours IST local time (~11:30 AM in Coordinated Universal Time (UTC)). We have utilised the upper 120 m of water column data: measured at an interval of 5 dbars between 200–10 dbars of depth and an interval of 1 dbars from 10 dbars of depth to the

surface. Since, the profiles were not uniform in vertical; they were linearly interpolated from the surface (1 m) to 120 m depth with a regular interval of 1 m. The gaps in C-Float data (on 10 October 2014 and 8 December 2016) were filled with linear interpolation to facilitate the analysis. The accuracies of pressure, temperature, salinity, chlorophyll-*a*, optical backscattering and dissolved oxygen sensors from C-Float are 2.4 dbars, 0.002°C, 0.005 psu, 0.015 mg m^{-3}, 0.0015 m^{-1}, and < 8 µM respectively. The temperature and salinity data are quality controlled by following *Wong et al.* [2015] and *Udaya Bhaskar et al.* [2012].

Though dissolved oxygen and chlorophyll measurements from the C-Float can produce highly stable data over longer duration, large biases were also been reported in the measurements made by the profiling floats. Hence, it is important to validate and correct any offsets in float measurements using independent *in situ* observations (water sample data). A detailed description of correction and validation of dissolved oxygen and chlorophyll measurements from the C-Float is given in the supporting information (S2) and (S3) respectively.

The C-Float used in this study does not possess any nitrate sensor. Hence, a BGC-Argo float (WMOID 5903712; hereafter N-Float (Nitrate-Float)) deployed by Monterey Bay Aquarium Research Institute (MBARI), USA, with 7-day temporal resolution with a nitrate sensor during September-December 2014 was identified. This N-Float was approximately 1° (~ 110 km) away from the C-Float location during TC *Hudhud* (the N-Float location is marked as a solid dark purple star in Figure 1). Although, the N-Float did not come under the direct influence of TC *Hudhud*, it provided a unique opportunity to understand the broad characteristics of the vertical structure of nitrate during this study period.

To estimate primary productivity (PP) integrated over the euphotic zone (z_{eu}), a well-known PP model of *Behrenfeld and Falkowski* [1997a] named as standard Vertically

Generalized Production Model (STD-VGPM) is used in this study. The STD-VGPM estimates vertical integrated PP over the Z_{eu} (PP_{zeu}^{Sat}) from the surface chlorophyll concentration, available light, and photosynthetic efficiency. Although, the STD-VGPM works well for estimating large scale spatial and temporal variability, a limitation of the STD-VGPM is its ignorance of the processes occurring over the water column. Since, the STD-VGPM was developed solely using surface data (mainly satellite), there were no accounting of the subsurface chlorophyll and temperature distribution. Hence, to address this issue, we modify the STD-VGPM to utilize vertical profiles of chlorophyll-*a* and temperature from BGC-Argo float to derive primary productivity profiles over the water column and defined it as $PP_z^{STD-VGPM-P}$. The integration of PP profile from surface to Z_{eu} provides values of vertically integrated PP from STD-VGPM-P ($PP_{z_{eu}}^{STD-VGPM-P}$). Supporting information (S4) gives a detailed description for the estimation of integrated PP upto the Z_{eu} based on primary productivity profiles obtained from STD-VGPM

The Ekman pumping velocity (positive for upwelling and negative for downwelling rate), at the base of the Ekman layer is estimated using the expression of *Fischer*, [1997] and *Girishkumar et al.* [2013b]. Mixed layer depth (MLD) is defined as the depth at which the σ_t (sigma-t) exceeds that at the surface with the increase in σ_t caused by a 1°C change in temperature [*Kara et al.*, 2000; *Girishkumar et al.*, 2012; *Thangaprakash et al.* 2016] and the isothermal layer depth (ILD) is defined as the depth where the temperature is 1°C lower than SST.

3. Results

3.1 The response of upper ocean temperature and salinity to TC *Hudhud* and TC *Vardah*

Temporal evolutions of physical and biogeochemical observations during the period of TC *Hudhud* and TC *Vardah* obtained from the C-Float are shown in Figure 2. Figure 3 shows temporal evolutions of SST, wind speed, OLR, Ekman pumping velocity and net surface heat flux averaged over a small domain encompassing C-Float locations (13.25°N–14°N and 88.45°E–89.25°E for TC *Hudhud* and 13.55°N–14.3°N and 86.2°E–87°E for TC *Vardah*; marked as brown box in Figure 4f and 4h respectively). Spatio-temporal evolutions of eight day averages of satellite measured SST and satellite chlorophyll before, during and after the period of TC *Hudhud* and TC *Vardah* are also presented in Figure 4.

Before the passage of TCs, temperature and salinity profiles obtained from C-Float showed typical hydrographic features during October–December in the BoB: warm and low salinity water in the near-surface layer, and cold and high salinity water in the subsurface layer [*Rao and Sivakumar,* 2000; *Rao and Sivakumar,* 2003; *Girishkumar et al.,* 2012; *Thangaprakash et al.,* 2016] (Figure 2a and 2b). Low wind speed and net surface heat flux into the ocean lead to warm (30°C) near-surface layer and a shallow ML (~10–30 m) during September–October 2014 and colder (29°C) and deeper ML (~40-70 m) during November 2016–January 2017. These features are consistent with the climatological characteristics of the BoB during fall and winter seasons [*Rao and Sivakumar,* 2000; *Thangaprakash et al.,* 2016] [Figures 2, 3 and 4]. The barrier layer (the difference between ILD and MLD), is weaker throughout study period (Figure 2b).

When TC *Hudhud* approached to the C-Float location, temperature showed a sudden decreasing tendency in the near-surface layers and this signature is clearly evident from 5

October 2014 onwards (Figure 2a and 3a). Further, near-surface salinity measurements from C-Float showed mild increasing tendency (~0.2 – 0.4 PSU) (Figure 2b). On 5 October 2014, the surface temperature was 29.6°C and it reduced to 27.1°C by 10 October 2014: the period during which TC *Hudhud* was closest to the C-Float location. Though, C-Float measurements showed only 2.5°C cooling in response to TC *Hudhud*, the daily satellite SST measurements showed much greater cooling (~4.5°C) during the same period (Figure 3a). Sub-sampling the daily satellite SST data to the C-Float temporal resolution reduces the magnitude of cooling to 3.7°C (from ~4.5°C). It clearly indicates that the coarser temporal resolution of the C-Float might be the primary reason for the underestimation of observed cooling magnitude (Figure 3a). Immediately after the passage of TC *Hudhud*, near surface temperature slowly recovered to the pre-cyclone period value (Figure 3a). However, the reduction in cooling is relatively much weaker during TC *Vardah* in comparison with TC *Hudhud* at the C-Float locations. During TC *Vardah,* C-Float (Satellite) measurements showed only 0.2°C (~1.5 °C) reduction in temperature. Moreover, the differences in temperature response between the TC *Hudhud* and TC *Vardah* are also evident from the spatio-temporal evolution of satellite SST: the cooling intensity was much larger along the track of TC *Hudhud* than TC *Vardah* (Figure 4). The SST started to recover from its cooling tendency immediately after the passage of TC *Hudhud* (27.1^{o}C on 10 October, 2014) and reached close to the pre-*Hudhud* value of 29.3^{o}C on 20 October 2014 after 10 days (on 5 October 2014, SST was 29.6°C) (Figure 2a and Figure 3a). Further, SST cooling associated with TC *Vardah* recovered within 5 days after the TC passage (Figure 3a).

Earlier studies have shown that the vertical processes, such as upwelling and entrainment due to wind-induced vertical mixing and convective overturning due to the net surface heat flux loss from the ocean are responsible for 70–80 % of SST cooling along the track of TC as compared with the lesser contribution from horizontal advection and enthalpy

flux (~20-30 %) [*Price* 1981; *Vincent et al.,* 2012a and 2012b; *Girishkumar et al.,* 2014]. Consistent with these earlier results, net surface heat loss from the ocean and horizontal advection played a weaker role on the observed SST cooling at C-Float location during TC *Hudhud* and TC *Vardah* (Figure S6). (See supporting information (S5) for relative role of horizontal advection and net surface heat flux on the observed SST cooling during TC period).

The analysis of temperature profiles on 05 October, 2014 (before TC *Hudhud*) and on 10 October, 2014 (during TC *Hudhud*) from C-Float shows cooling and deepening of isothermal layer due to the relative contribution from upwelling and vertical mixing (Figure 5). The temperature profiles in the upper 150 m of water column were cooled after the passage of TC *Hudhud* and this is the typical response to strong upwelling induced by the TC as documented in the earlier studies [*Park et al.,* 2011; *Sanford et al.,* 2011; Figure 12 b of *Zang et al.,* 2016]. Moreover, the presence of subsurface cooling after the passage of TC *Hudhud* also indicates the predominant role of upwelling rather than vertical mixing [*Zang et al.,* 2016]; strong upwelling tendency was observed on 9 October, 2014 (~10 m day^{-1}) at the C-Float location from the satellite data (Figure 3c). Earlier studies have shown the presence of strong near-inertial oscillations of upwelling and downwelling after the passage of TCs (*Price,* 1981; *Wang et al.,* 2012; *Park et al.,* 2011; *Sanford et al.,* 2011; *Zang et al.,* 2016). The near-inertial oscillation of upwelling can facilitate entrainment of cold thermocline water to the surface mixed layer [*Sanford et al.,* 2011; *Girishkumar et al.,* 2014; *Zang et al.,* 2016]. At 14°N (near to the C-Float location in the BoB), the theoretical inertial period is around 50 hours (~2 days). Hence, it is not possible to document the contribution of near-inertial oscillation on the observed responses using the C-float observations which having a temporal resolution of 5 days. Before TC *Hudhud,* near surface temperature structure shows nearly uniform temperature (29.6 °C) up to the depth of 25 m and the position of 27 °C isotherm

was at the depth around 50 m. When TC was nearest to the C-Float location, isothermal layer got deepened and near surface temperature drops to 27°C in response to the strong TC induced-upwelling and vertical mixing. As suggested by *Sengupta et al.* [2008], we assume that TC induced vertical mixing penetrates vertically upto the intersection of pre and post-storm sigma-t profiles below the isothermal layer. The sigma-t and temperature profile before and after the TC *Hudhud* intersects around 50 m (Figure 5a and 5b). Hence, we can assume that the vertical extent of the mixing was up to the upper 50 m of the water column (Figure 5a and 5b).

Similarly, before the approach of TC *Vardah*, near surface temperature structure from C-Float shows nearly uniform temperature (28.9 °C on 3 December 2016) up to the depth of 45–50 m. As the TC *Vardah* crosses closest to the C-Float locations, near surface temperature drops to 28.7^{o}C and isothermal layer got deepened to 60 m. Moreover, the sigma-t profiles before and after the TC *Vardah* intersect at depth of 60 m. Hence, we can assume that the vertical extent of the TC *Vardah* mixing was up to the upper 60 m of the water column (Figure 5c and 5d).

3.2. Enhancement of nitrate at the near surface layer in response to TC *Hudhud* and TC *Vardah*

The nitrate profile from the profiling float during October–December 2014 shows oligotrophic conditions in the near surface layer with the nutricline (defined as 2.5 µM) situated around 40–60 m depth (Figure 6). Moreover, strong temporal correspondence between ILD and upper part of nutricline were also been observed [Figure 6]. Following the method proposed by *Son et al.* [2007], we made a simple estimation of the upward flux of nitrate in response to the TC forcing. Since, nutricline depth and ILD shows strong temporal

correspondence, we utilized nitrate profiles from N-Float having close resemblance with pre-TC temperature profiles from the C-Float (*Supplementary section S7 gives a detailed description of selection of vertical profiles of nitrate to estimate vertical flux of nitrate)*. Our analysis suggests that there is an approximate increase of 6.6 µM (2.3 µM) in the nitrate concentration in the upper layer in response to TC *Hudhud* (TC *Vardah).* We assumed that the integrated nitrate concentration from the surface to the 50 m (60 m) water depth is equally distributed in the vertical during TC *Hudhud* (TC *Vardah*). The estimation of nitrate concentration enhancement in the near surface layer in response to TC *Hudhud* is consistent with the result of *Naik et al.* [2008]. From the ship based *in situ* observations, *Naik et al.* [2008] have reported an enhancement of 5 µM in the nitrate concentration in the near surface layer after the passage of a TC in the Arabian Sea. Similarly, *Jayalakshmi et al.* [2013] have also reported the increase of 3.8 µM in nitrate concentration at a cyclonic eddy region in the south western BoB during northern winter.

It is worth noting that the values of the wind and net surface heat flux reverted back to their pre-TC period values immediately after the passage of TC *Hudhud* and TC *Vardah* at the C-Float location (Figure 3b, and 3d). This suggests that upward flux of nutrients into the near-surface layer might have stopped within this time. Hence, we can safely assume that the enhancement of nitrate concentration in the near-surface layer happened only during the period when TC was close to the float location.

3.3. The upper ocean chlorophyll and optical backscatter response to TC *Hudhud* and TC *Vardah*

Temporal evolution of depth-time section of chlorophyll-*a* data obtained from the C-Float showed a persistent occurrence of subsurface chlorophyll maxima (0.8–1.2 mg m^{-3}) at around 30–80 m depth throughout the study period except few days after passage of TC *Hudhud* and TC *Vardah* (Figure 2c). The persistent occurrence of subsurface chlorophyll

maxima observed during the study period is the net result of optimum availability of both the light and the nutrients at that particular depth [*Brock et al.,* 1993; *Huisman et al.,* 2005; *Naik et al.,* 2008; *Ravichandran et al.,* 2012]. The growth of phytoplankton primarily depends on light and nutrients: light decreases exponentially and nutrients increase as depth increases. Consistent with oligotrophic characteristics observed in the vertical distribution of nitrate profile (Figure 6), chlorophyll concentration in the near-surface layer (upper 40–60 m) was also very small (0.15 mg m^{-3}) before TC period (Figure 2c). When TC *Hudhud* (TC *Vardah*) approached to the C-Float location, chlorophyll concentration during 5 October 2014 (3 December 2016) in the near surface layer gradually increased from 0.15 (0.12) mg m^{-3} and reached to the maximum value of 3.6 mg m^{-3} (1.5 mg m^{-3}) during 20 October 2014 (18 December 2016) (Figure 2c and Figure 3e; black line). Interestingly, strong increasing tendency of chlorophyll concentration in the near surface layer persisted up to 10 (15) days after the passage of TC *Hudhud* (TC *Vardah*) at the C-Float location in the BoB. Similar to the temperature response, observed chlorophyll enhancement in response to TC *Hudhud* were much higher (~2.5 times) than TC *Vardah.*

It is interesting to note that, the temporal evolution of the chlorophyll response was in contrast with that of the SST response such that enhancement of the chlorophyll persisted even after 10 (15) days from the passage of TC *Hudhud* (TC *Vardah*), that is chlorophyll started to recover to its pre-cyclonic values much slower than SST (Figure 2 and 3).

The enhancement of chlorophyll concentration and its persistence was clearly apparent from the 7-days averages of chlorophyll along the TC track after the life cycle of TC *Hudhud* (8–14 October, 2014 and TC *Vardah* (8–14 December, 2016) (Figure 4e and 4g). However, the cold wake generated along the track disappeared almost immediately after the life cycle of TC and this is clearly evident in the 7-days average (15–21 October, 2014 and 15–21 December, 2016) of MW-OISST (Figure 4j and 4l).

Plausible factors that modulated the enhancement and persistence of chlorophyll, even after the passage of TC are examined. Enhancement of chlorophyll in the near-surface layer during TC is primarily caused by TC induced vertical mixing. Enhancement of chlorophyll depends upon the following two factors: new production of chlorophyll as a result of increased nutrient supply from subsurface waters and the upward flux of chlorophyll from sub-surface chlorophyll-rich waters [*Vinayachandran et al.,* 2005; *Ravichandran et al.,* 2012].

However, increase in nitrate concentration does not lead to immediate rapid increase in chlorophyll concentration during the period of TC and it is clearly evident from the depth integrated chlorophyll in the upper 400 m of water column (Figure 7a). The reason for the selection of 400 m depth is primarily due to the low chlorophyll concentration along with absence of any significant trend at this depth. However, our conclusion is still valid irrespective of the actual depth level chosen (from 60 m to 400 m depth level) for the vertical integration of chlorophyll (Table-S5). The integrated chlorophyll in the upper 400 m shows an enhancement of 40 mg m^{-2} over 10 days during 5–15 October 2014. However, within next 5 days (during 15–20 October, 2014) depth integrated chlorophyll concentration increased to 70 mg m^{-2}, which is approximately 1.75 times higher than enhancement with respect to previous 10 days (Figure 7a; Table-S5). From 20–25 October 2014, integrated chlorophyll shows sudden drop in the upper 400 m of the water column and returns to its pre-TC (before TC *Hudhud)* conditions around 30 October 2014 (Figure 7a; Table-S5). Similarly, integrated chlorophyll in the upper 400 m of water column shows an enhancement of 16 mg m^{-2} during 3–13 December 2016 and an increase of almost similar magnitude were observed in the subsequent two pentads (13–18 December 2016 and 18–23 December 2016) as a response to TC *Vardah* and returns to pre-*Vardah* period by 28 December 2016.

In order to understand the relative contribution of the upward flux of chlorophyll rich

sub-surface water on the observed enhancement of chlorophyll in the near surface layer in response to TC, we made a rough estimation of the upward flux of chlorophyll by mixing. As discussed above, the upward fluxes of subsurface chlorophyll into the near-surface layer took place only during the period of strong wind induced vertical mixing and upwelling associated with TC *Hudhud* and TC *Vardah*. Integrated chlorophyll concentration between the layers 0–400 m and 0–60 m during 5 October 2014 and 10 October 2014 shows an enhancement of 20 mg m^{-2} and 26.5 mgm^{-2} respectively where a reduction of 6.5 mg m^{-2} chlorophyll concentration at the layer 60–400 m (the selection of 60 m depth is based on the signature of chlorophyll concentration in the upper 60 m of water column in response to TC) (Table- S6). It indicates that approximately 20-24 % increase in chlorophyll concentration at the near-surface layer was contributed by the upward flux of sub-surface chlorophyll maxima into the near-surface layer in response to TC *Hudhud.* Similar estimation during TC *Vardah* indicates upward flux of sub-surface chlorophyll lead to approximately 22-30 % of surface bloom (Table-S6). Moreover, both the wind and the net surface heat flux reached their pre-cyclone conditions immediately after the TC period at the C-Float location (12 October 2014 for TC *Hudhud* and 10 December 2016 for TC *Vardah*) (Figure 3b and 3d). The vertical chlorophyll flux calculation will be sensitive to the exact choice of water column. However, estimation of vertical chlorophyll for a range of depths (100 to 400 m) indicates that the results do not change greatly, with a maximum contribution of 20–24 % during TC *Hudhud* and 22–30 % during TC *Vardah* (Table-S6).

In addition to the enhancement of near surface chlorophyll through the upward flux of chlorophyll, there might be some contribution by the horizontal advection of chlorophyll into the study region. Both horizontal advection and upward flux of chlorophyll simply move the pigment across the gradient, hence, we cannot consider the chlorophyll enhancement as new primary production or carbon export associated with these processes. However, spatial

distribution of chlorophyll from satellite data does not show any evidence of chlorophyll enhancement, except along the track of TC. It clearly negates the role of horizontal advection on the observed enhancement of chlorophyll in response to both the TCs.

It is interesting to note that, during the period of intense chlorophyll bloom at the near- surface layer, sub-surface chlorophyll maxima were absent (Figure 2c). This might be due to the presence of large cloud cover and reduction in the downward penetration of solar radiation in the water column due to large quantities of chlorophyll in the near surface layer. This is clearly evident from the euphotic depth evolution which shallows during the period of TC as compared to the pre-TC period (Figure 2c; pink line).

We have also examined the particulate backscattering at 700 nm wavelength from the C-Float (Figure 2e and 3e), which provides indirect information about total particulate matter including chlorophyll-*a*. Recent studies show that there is an existence of strong relationship between phytoplankton biomass and particulate backscattering in the absence of suspended inorganic sediment at the near surface layer of the open ocean region *Martinez-Vincente et al*. [2014] and *Graff et al.* [2015]. Hence, the backscatter signal may also be considered as a proxy for phytoplankton biomass in the open ocean along with chlorophyll fluorescence. The location of C-Float used in this study is far away from any river mouth and hence the possibility of suspended inorganic sediments signal on optical backscatter measurements can be ignored. Our analysis shows strong temporal correspondence between chlorophyll fluorescence and particulate backscattering. This clearly shows that the C-Float observed chlorophyll fluorescence signals are not just physiological responses of the phytoplankton to the variations in light due to TC induced cloud cover.

3.4. The response of upper ocean primary productivity (PP) to TC *Hudhud* and TC *Vardah*

We compared the estimated $PP_{z_{eu}}^{STD-VGPM-P}$ based on chlorophyll and temperature profile from C-Float (Figure 8a; green line) with: (i) PP derived from satellite (PP_{zeu}^{Sat}) using merged chlorophyll-*a* (mg m^{-3}) and MW-OI SST (°C) (Figure 8a; red line), and (ii) PP derived from the C-Float (PP_{zeu}^{Surf}) surface chlorophyll (mg m^{-3}) and surface temperature (°C) (Figure 8a; black line). During the study period, the temporal evolution of the $PP_{z_{eu}}^{STD-VGPM-P}$ shows reasonable good agreement with both PP_{zeu}^{Sat} and PP_{zeu}^{Surf}. However, the estimated peak magnitude of $PP_{z_{eu}}^{STD-VGPM-P}$ is lower than PP_{zeu}^{Surf}, after the TC forcing period (Figure 8). As suggested by *Hemsley et al.* [2015], this discrepancy in *PP* might be associated with the contribution from subsurface chlorophyll maxima, which could be resolved only by the C-Float observations. In general, temporal evolution of the *PP* shows similar trend as the temporal evolution of chlorophyll in response to TC (Figure 2c, 8a and 8c). In the subsequent discussion, $PP_{z_{eu}}^{STD-VGPM-P}$ (Figure 8a; green line) is referred as PP for simplicity.

Before TC period, *PP* was estimated as 0.2 g C m^{-2} day^{-1} (Figure 8a; green line) and it got increased to 1.9 g C m^{-2} day^{-1} (during 20 October 2014) in response to TC *Hudhud* forcing (Figure 8a; green line) which is consistent with temporal evolution of chlorophyll. By 25 October 2014, there was a sharp decrease in PP and reached to pre-*Hudhud*-period values (0.2 g C m^{-2} day^{-1}). This indicates that average new production in the euphotic depth during 10–20 October 2014 is approximately 1.5 g C m^{-2} day^{-1}. As discussed in the previous section, if we consider 24 % increase in the chlorophyll concentration in the near-surface layer which is contributed by the upward flux of sub-surface chlorophyll maxima into the near-surface layer, then new primary production is increased to 1.2 g C m^{-2} day^{-1} in response to TC *Hudhud*. Also, as discussed in the previous section, the enhanced nitrate (6.6 µM)

concentration due to TC *Hudhud* added to the upper 50 m of the water column was completely utilized within 15 days (5–20 October 2014). Then as per canonical Redfield Ratio, the average new production would be ~1.7 g C m^{-2} day^{-1}, which is in close agreement with estimated new production (1.2 g C m^{-2} day^{-1}).

In response to TC *Vardah*, PP started to increase from 0.2 g C m^{-2} day^{-1} on 3 December 2016 and attained maximum value of 0.95 g C m^{-2} day^{-1} during 18 December 2016. The high values of PP were maintained in the next two pentads and it started to decrease sharply by 28 December 2016. Hence, the average new production at the euphotic depth during 8–28 December 2016 before (after) removing the contribution of 24% of vertical flux of chlorophyll is approximately 0.75 g C m^{-2} day^{-1} (0.60 g C m^{-2} day^{-1}). This estimation is in agreement with the average new production of 0.55 g C m^{-2} day^{-1}, if complete utilization of 2.3 µM nitrate in the upper 60 m of water column within 20 days (3-23 December 2016) is assumed.

3.5. The response of upper ocean dissolved oxygen to the TCs *Hudhud and Vardah*.

During pre- and post-TC period, temporal evolution of the vertical profiles of dissolved oxygen concentration showed peak values (> 210 µM) in the upper 30 m of the water column. The OMZ (< 22 µM) was observed below 80 m depth (Figure 2d). Moreover, the strong vertical gradient in dissolved oxygen concentration (defined as oxycline) was observed around 50–80 m depth and it shows strong temporal correspondence with the thermocline (Figure 2). In response to TC *Hudhud*, the dissolved oxygen concentration at 30–35 m depth decreased from 200 µM to as low as 140 µM (31 % saturation) on 15 October 2014 (Figure 2d and 7c). The intrusion of subsurface water with low concentration of oxygen due to the strong wind induced vertical mixing and upwelling associated with TC must be the most plausible explanation for the reduction in the near surface layer oxygen concentration.

The strong temporal correspondence between outcropping of 27°C isotherm and 175 µM dissolved oxygen contour (Figure 2d; purple line) provides clear evidence of the intrusion of subsurface water with low concentration of oxygen into near surface layer.

The enhancement of oxygen in the near surface layer was observed during 15–20 October 2014, with maximum value (238 µM) during 20 October 2014, which is approximately 25 µM higher than pre-*Hudhud* period (Figure 2d and 7c). Please note that the enhancement of oxygen in the near surface layer lead to increase in oxygen super saturation condition from 111 % to 123 % (~12 % increase).

Moreover, mild increasing tendency in dissolved oxygen concentration were also observed after the passage of TC *Vardah* on 23 December, 2016 in the near surface layer. Overall, consistent with temperature and chlorophyll responses, dissolved oxygen response were comparatively lower in magnitude during the TC *Vardah* as compared with the dissolved oxygen response during the TC *Hudhud* period. Similar enhancement of oxygen observation in response to increasing chlorophyll concentration due to a TC in the South China Sea was reported by *Lin et al.* [2014]. The entrainment of oxygen from the overlying air due to the strong winds can lead to the enhancement of dissolved oxygen in the near-surface layer. However, observation shows weaker winds during the period of enhancement of oxygen in the near-surface layer after the passage of TC *Hudhud* and TC *Vardah* (Figure 3b and 7c). Hence, the enhancement of oxygen in the near surface layer must be a consequence of enhancement of photosynthetically produced oxygen due to chlorophyll concentration enrichment in the near surface layer in response to the TC *Hudhud.*

4. Plausible causative mechanism of the differential oceanic response during TC *Hudhud* and TC *Vardah* at the C-Float location

Both satellite wind speed and maximum sustained surface wind speed from the best track data shows relatively higher values when TC *Vardah* (17 m s^{-1}) was close to the C-Float location as compared to the TC *Hudhud* (15 m s^{-1}) period (Table-1): implying stronger forcing during TC *Vardah* as compared to TC *Hudhud*. However, the observed oceanic response to the TC *Vardah* is weaker when compared to TC *Hudhud*. A plausible mechanism for observed differential response is the different translational speeds of the TCs *Vardah* and *Hudhud*. As reported earlier [*Dare and Mcbride,* 2011; *Mei et al.*, 2012; *Lin* 2013], due to high translation speed, a TC can traverse without significantly disturbing the underlying ocean. The estimated translation speed (using IMD best track data) of TC *Vardah* was significantly higher (5 ms^{-1}) than TC *Hudhud* (2 ms^{-1}), when they are crossing over the C-Float locations (Tabel-1). Hence, this translational speed difference plays a significant role for the weak oceanic responses during the TC.

In addition to the difference in translation speeds, presence of cold core (cyclonic) eddy can also play a critical role in modulating the TC induced physical and biogeochemical oceanic responses. The presence of cyclonic eddy lifts thermocline and nutricline, thus turbulent mixing can lead to entrainment of cold and nutrient rich subsurface water to near surface layer effortlessly in comparison with in the case of no eddy/or warm core (anti-cyclonic) eddy [*Falkowski et al.,* 1991*; Prasanna Kumar et al.,* 2004; *Shang et al.,* 2008; *Ravichandran et al.,* 2012; *Wang et al.,* 2016]. The analysis of sea surface height (SSHA) data at the C-Float location during the study period indicates the presence of a pre-existing cold core eddy (negative SSHA) before the passage of TC *Hudhud* and a warm core eddy (positive SSHA) before the passage of TC *Vardah* [Figure 9]. Consistent with SSHA signature before the passage of TC's, thermocline was deeper during TC *Vardah* as compared

to TC *Hudhud* (Figures 2 and 9). The evolution of temperature profile in response to TC *Hudhud* (TC *Vardah*) is a typical response of temperature profile in response to TC in the presence of cyclonic eddy (anticyclonic eddy) (cf. Figure 6 of *Pan and Sun* [2013]). Considering the close correspondence of nutricline and ILD, it is worth speculating that before the passage of TC, the nutricline during the TC *Hudhud* might be shallow than that during TC *Vardah*. During the TC *Hudhud* forcing, the presence of pre-existing shallow nutricline and thermocline may lead to much freer turbulent exchange of nutrient rich subsurface cold water to near surface layer and it may lead to higher SST cooling and chlorophyll enhancement in comparison with TC *Vardah*.

Another influence of a cold core eddy is to trap near-inertial oscillations induced by TC in the ML [*Jaimes et al.,* 2011]. This increases vertical shear and entrainment at the base of mixed layer, which in turn increases the upper ocean response to TC as it was observed in the case of TC *Hudhud*. In contrast, the presence of warm core eddy allows rapid vertical dispersion of near-inertial energy and it reduces the shear and mixing at the base of mixed layer and which in turn lead to less upper ocean response as observed in the TC *Vardah* [*Jaimes et al.,* 2011].

It is worth noting that the present analysis does not quantify the relative contributions of translation speed and pre-existing eddy field on the observed differential oceanic response between TC *Hudhud* and TC *Vardah*. Numerical simulations can provide more insights on this topic.

6. Summary

In situ observations of temperature, salinity, chlorophyll-*a*, optical backscatter and dissolved oxygen from a Biogeochemical-Argo float (C-Float) are used to understand the

complex biophysical interactions during two strong TC forcing events. Though wind speed magnitude was higher during the TC *Vardah* (17 m s^{-1}) compared to the TC *Hudhud* (15 m s^{-1}), the oceanic response to the TC *Vardah* was much weaker compared to the TC *Hudhud.* The availability of good quality *in situ* observations from the same C-Float during these two TC events provides an opportunity not only to document the complex bio-physical oceanic responses but also to identify plausible reasons for the observed difference in the oceanic responses during these two TC events.

Our analysis shows a significant reduction in sea surface temperature (SST) (~2.5 °C) along with the significant enhancement of nitrate (~ 6.6 µM) and chlorophyll concentrations (3.6 mg m^{-3}) in the near surface layer of the water column in response to the TC *Hudhud* induced vertical mixing. However, during the TC *Vardah* period, SST was reduced by 0.2 °C only with a weaker enhancement of nitrate (2.3 µM) and chlorophyll (1.5 mg m^{-3}) concentrations. During the TC *Hudhud* period, the integrated chlorophyll concentration in the upper 60 m of the water column increased approximately by 4.5 times (35 mg m^{-2} to 160 mg m^{-2}) with respect to the pre-TC *Hudhud* with peak intensity occurring around 10 days after the passage of TC. However, during TC *Vardah*, the enhancement of chlorophyll in the upper 60 m of the water column was only increased by 2 times (39 mg m^{-2} to 80 mg m^{-2}) with respect to the pre-TC *Vardah* with maximum intensity around 15 days after the passage of TC. Though the peak intensity of enhanced chlorophyll occurred only after 10-15 days from the passage of TC, SST started to recover immediately after the passage of TC. Our analysis further showed that approximately 24-30 % increase in the chlorophyll concentration at the near surface layer was contributed by the upward flux of sub-surface chlorophyll maxima into the near surface layer during the initial period of enhancement of chlorophyll. Our analysis further suggests that, the enhancement of chlorophyll in the near surface layer leads

to the increase in integrated primary production in the euphotic zone from 0.2 g C m^{-2} day^{-1} to 1.9 g C m^{-2} day^{-1} (0.95 g C m^{-2} day^{-1}) in response to the TC *Hudhud* (TC *Vardah*).

Strong vertical mixing and upwelling associated with the TC *Hudhud* caused intrusion of lower dissolved oxygen subsurface waters into the near-surface layers, leading to strong decreasing tendencies in dissolved oxygen concentration between 30-35 m of water column. When the TC *Hudhud* was nearest to the C-Float, the dissolved oxygen concentration at the 35 m depth decreased to as low as to 140 µM (31 % saturation) in comparison with the pre-*Hudhud* dissolved oxygen concentration of 200 µM. Further, the enhancement of oxygen in the near-surface layer in the upper 20 m of water column were also observed approximately 10 days after the passage of TC *Hudhud*. During this period, dissolved oxygen concentration increased to 238 µM, which is approximately 25 µM higher than the dissolved oxygen concentration before TC *Hudhud* period. This enhancement of oxygen in the near surface layer leads to increase in oxygen super saturation condition from 111 % to 123 % (~12 % increase). Our analysis suggests that the enhancement of oxygen in the near-surface layer is a consequence of enhancement of photo-synthetically produced oxygen due to increased chlorophyll concentration at the near-surface layer in response to the TC *Hudhud*. However, dissolved oxygen response is barely noticeable during the TC *Vardah* period.

In summary, our analysis suggests that the relatively smaller (higher) translation speed and presence of a cold (warm) core eddy lead to stronger (weaker) oceanic responses at the C-Float location in response to the TC *Hudhud* (TC *Vardah*). Moreover, the present study emphasizes that to accurately simulate the biogeochemical responses to the TC forcing in coupled-biophysical ocean models is contingent upon the accurate representation of both the physical and dynamical state of the background oceanic structure and storm characteristics.

Acknowledgement

The encouragement and facilities provided by the Director, INCOIS are gratefully acknowledged. We thank three anonymous reviewers for their help in improving the manuscript substantially. Argo floats were collected and made freely available by the International Argo Program and the national programs that contribute to it (http://www.argo.ucsd.edu, http://argo.jcommops.org). The Argo Program is part of the Global Ocean Observing System (Argo (2000). BGC-Argo floats data and metadata from Global Data Assembly Centre (Argo GDAC SEANOE. http://doi.org/10.17882/42182). OLR dataset is provided by Indian Institute of Tropical Meteorology (IITM), Pune, India. C-*2015* ASCAT data are produced by Remote Sensing Systems and sponsored by the NASA Ocean Vector Winds Science Team. ASCAT data were obtained from the Centre de RechercheetdExploitationSatellitaire (CERSAT), at IFREMER, Plouzané (France) and distributed through Asia Pacific data research center (APDRC; http://apdrc.soest.hawaii.edu/datadoc/ascat.php).The altimeter products are distributed by E.U. Copernicus Marine Service Information (CMEMS). The TropFlux data is produced under a collaboration between Laboratoired'Océanographie: ExpérimentationetApprochesNumériques (LOCEAN) from Institut Pierre Simon Laplace (IPSL, Paris, France) and National Institute of Oceanography/CSIR (NIO, Goa, India), and supported by Institut de Recherche pour le Développement (IRD, France). GlobColour data (http://globcolour.info) used in this study has been developed, validated, and distributed by ACRI-ST, France. Microwave OI SST data are produced by Remote Sensing Systems and sponsored by National Oceanographic Partnership Program (NOPP) and the NASA Earth Science Physical Oceanography Program. The authors also thank Mr. Rajasekhar, Vessel Management Cell, National Institute of Ocean Technology (NIOT), Chennai and the Captain and crew of ORV Sagar Nidhi for facilitating the SN-120 field measurements successfully.

Graphics were generated using PyFerret. This is INCOIS contribution number XXX.

References

Alam, Md. M., Md. A. Hossain, and S. Shafee (2003), Frequency of Bay of Bengal cyclonic storms and depressions crossing different coastal zones, *Int. J. Climatol.*, 23, 1119–1125, doi:10.1002/joc.927.

Behrenfeld, M. J., P. G. Falkowski (1997a), Photosynthetic rates derived from satellite-based chlorophyll concentration, *Limnol. Oceanogr.*, 42, 1-20.

Behrenfeld, MJ, P. G. Falkowski (1997b), A consumer's guide to phytoplankton primary productivity models, Limnol. Oceanogr., 42, 1479-1491.

Bentamy, A., and C-F. Denis (2012), Gridded surface wind fields from Metop/ASCAT measurements, *Int. J. Remote.*, 33(6), 1729-1754. doi:10.1080/01431161.2011.600348.

Boss, E. B. and N. Haëntjens, (2016), Primer regarding measurements of chlorophyll fluorescence and the backscattering coefficient with WETLabs FLBB on profiling floats. SOCCOM Tech. Rep. 2016-1.

Brock, J., S. Sathyendranath, and T. Piatt (1993), Modelling the seasonality of subsurface light and primary production in the Arabian Sea, *Mar. Ecol. Prog. Ser.*, 101, 209-221.

Catherine, S., ClaustreHerve., Poteau Antoine., and D OrtenzioFabrizio (2014). Bio-Argo quality control manual for Chlorophyll-*a* concentration, Version 1, doi: 10.13155/35385.

Chacko N., **(**2017), Chlorophyll bloom in response to tropical cyclone Hudhud in the Bay of Bengal: Bio-Argo subsurface observations, Volume 124, June 2017, Pages 66–72, https://doi.org/10.1016/j.dsr.2017.04.010

Chang, Y., J. W. Chan, Y. C. A. Huang, W. Q. Lin, M. A. Lee, K. T. Lee, C. H. Liao, K. Y. Wang, and Y. C. Kuo (2014), Typhoon-enhanced upwelling and its influence on fishing activities in the southern East China Sea, *Int. J. Remote Sens.*, 35(17), 6561–6572, doi: 10.1080/01431161.2014.958248

Chen, X., D. Pan, Y. Bai, X. He, C. A. Chen, and Z. Hao (2013), Episodic Phytoplankton Bloom Events in the Bay of Bengal Triggered by Multiple Forcings, *Deep-Sea Res. II*,73, 17–30, doi:10.1016/j.dsr.2012.11.011.

Chung, C. C., G. C. Gong, and C. C. Hung (2012), Effect of Typhoon Morakot on Microphytoplankton Population Dynamics in the Subtropical Northwest Pacific, *Marine Ecology Progress Series*, 448, 39–49, doi:10.3354/meps09490.

Currie, J. C., M. Lengaigne, J. Vialard, D. M. Kaplan, O. Aumont, S. W. A. Naqvi, and O. Maury (2013), Indian Ocean Dipole and El Niño/Southern Oscillation impacts on regional chlorophyll anomalies in the Indian Ocean, *Biogeosciences*, 10, 6677–6698, doi:10.5194/bg-10-6677-2013.

Deuser, W.G. (1975), Reducing environments, *Chemical Oceanography*, 3, 2nd ed., pg.1-37.

Ducklow, H. W., D. K. Steinberg, and K. O. Buesseler (2001), Upper ocean carbon export and the biological pump, *Oceanography*, 14, 50–58.

Ekau, W., H. Auel, H. O. Portner, and D. Gilbert (2010), Impacts of hypoxia on the structure and processes in pelagic communities (zooplankton, macro-invertebrates and fish), *Biogeoscience*, 7, 1669-1699, doi:10.5194/bg-7-1669-2010.

Falkowski, P. G., D. Ziemann, Z. Kolber, and P. K. Bienfang, (1991), Role of eddy pumping in enhancing primary production in the ocean," Nature, vol. 352, no. 6330, pp. 55–58.

Fantond'Andon, O., A. Mangin, S. Lavender, D. Antoine, S. Maritorena, A. Morel, and G. Barrot (2009), "GlobColour - the European Service for Ocean Colour", *in Proceedings of the 2009 IEEE International Geoscience & Remote Sensing Symposium, Jul 12-17 2009, Cape Town South Africa: IEEE Geoscience and Remote Sensing Society.*

Fiedler P.C., J. V. Redfern, N. J. Van, C. Hall, R. L. Pitman, and L. T. Ballance (2013), Effects of a tropical cyclone on a pelagic ecosystem from the physical environment to top predators, *Marine Ecology Progress Series*, 484, 1–16, doi: 10.3354/meps10378.

Fischer, A. S. (1997), Arabian Sea mixed-layer deepening during the monsoon: Observations and dynamics, S.M. thesis, 130 pp., Mass. Inst. Of Technol. and Woods HoleOceanogr. Inst., Woods Hole, Mass.

Gentemann, C., C.J. Donlon, A. Stuart-Menteth, and F.J. Wentz (2003), Diurnal signals in Satellite Sea surface temperature measurements, *Geophys. Res. Lett.*, 30(3):1, 140–1, 143, http://dx.doi.org/10.1029/2002GL016291.

Wang, G., L. Wu, N. C. Johnson, and Z. Ling (2016), Observed three-dimensional structure of oceancooling induced by Pacific tropical cyclones, Geophys. Res. Lett.,43, 7632–7638, :10.1002/2016GL069605

Girishkumar M. S., K. Suprit, J. Chiranjivi, TVS. Udaya Bhaskar, M. Ravichandran, R. VenkatShesu, E. Pattabhi Rama Rao (2014), Observed Oceanic response to tropical cyclone Jal from a moored buoy in the south-western Bay of Bengal, *Ocean Dynam.*, 64, 325–335, doi:10.1007/s10236-014-0689-6.

Girishkumar, M. S., K. Suprit, S. Vishnu, V. P. Thangaprakash and M. Ravichandran (2015), The role of ENSO and MJO on rapid intensification of Tropical Cyclones in

the Bay of Bengal during October-December, *Theor. Appl. Climatol.*, 120: 797. doi:10.1007/s00704-014-1214-z.

Girishkumar, M. S., M. Ravichandran, and M. J. McPhaden, R. R. Rao (2011), Intraseasonal variability in barrier layer thickness in the south central BoB, *J. Geophys. Res., Ocean,*116, C03009, doi: 10.1029/2010JC006657.

Girishkumar, M. S., M. Ravichandran, and V. Pant (2012), Observed chlorophyll-a bloom in the southern Bay of Bengal during winter 2006–2007, *Int. J. Remote Sens.*, 33(4), 1264-1275, doi: 10.1080/01431161.2011.563251.

Girishkumar, M. S., M. Ravichandran, and W. Han (2013b), Observed intraseasonal thermocline variability in the Bay of Bengal, J. Geophys. Res. Oceans, 118, 3336–3349, doi:10.1002/jgrc.20245.

Girishkumar, M. S., M. Ravichandran, and M. J. McPhaden (2013a), Temperature inversions and their influence on the mixed layer heat budget during the winters of 2006–2007 and 2007–2008 in the Bay of Bengal, *J. Geophys. Res. Oceans*, 118, 2426–2437, doi:10.1002/jgrc.20192.

Gomes, H. R., J. I. Goes, T. Saino (2000), Influence of physical processes and freshwater discharge on the seasonality of phytoplankton regime in the Bay of Bengal, *Cont. Shelf Res.*, 20, 313– 330.

Gomes, H. R., S. deRada, J. I. Goes, and F. Chai (2016), Examining features of enhanced phytoplankton biomass in the Bay of Bengal using a coupled physical-biological model, *J. Geophys. Res. Oceans*, 121, 5112–5133, doi:10.1002/2015JC011508.

Graff, J. R., T. K. Westberry, A. J. Milligan, M. B. Brown, G. Dall'Olmo, V. van Dongen-Vogels, K. M. Reifel, and M. J. Behrenfeld (2015), Analytical phytoplankton carbon measurements spanning diverse ecosystems, *Deep Sea Res., Part I*, **102**, 16–25, doi:10.1016/j.dsr.2015.04.006.

Hemsley, V. S., T. J. Smyth, A. P. Martin, E. Frajka-Williams, A. F. Thompson, G. Damerell, and S. C. Painter (2015), Estimating Oceanic Primary Production Using Vertical Irradiance and Chlorophyll Profiles from Ocean Gliders in the North Atlantic, *Environmental Science and Technology*, 49(19), DOI: 10.1021/acs.est.5b00608·

Huisman, J., P. N. N. Thi, D. M. Karl, and B. P. Sommeijer (2006), Reduced mixing generates oscillations and chaos in the deep chlorophyll maximum, *Nature*, 439, 7074:322-5, doi: 10.1038/nature0424.

Hung, C. C., G. C. Gong, W. C. Chou, C. C. Chung, M. A. Lee, Y. Chang, H. Y. Chen, S. J. Huang, Y. Yang, W. R. Yang, W. C. Chung, S. L. Li, and E. Laws (2010), The Effect of Typhoon on Particulate Organic Carbon Flux in the Southern East China Sea, *Biogeosciences*, 7, 3007–3018, doi:10.5194/bg-7-3007-2010.

Jacox, M. G., Chrostopher A. Edwards, Matikahru, Daniel L. Rudnick, and Raphael M. kudela (2013), The potential for improving remote primary productivity estimates through subsurface chlorophyll and irradiance measurements, *Deep sea Research II*, 112, 107-116, http://dx.doi.org/10.1016/j.dsr2.2013.12.008.

Jayalakshmi, K. J., P. Sabu, C. R. Devi, and V. N. A. Sanjeevan (2015), Response of micro- and mesozooplankton in the southwestern Bay of Bengal to a cyclonic eddy during the winter monsoon 2005, *Environ.Monit.Assess.*, 187, 473, doi:10.1007/s10661-015-4609-0.

Kara, A. B., P. A. Rochford, and H. E. Hurlbutt (2000), Mixed layer depth variability and barrier layer formation over the North Pacific Ocean, *J. Geophys. Res.*, *Oceans*, 105(C7), 16783–16801, doi: 10.1029/2000JC900071.

Kobayashi, T., T. Suga, and N. Shikama (2006), Negative bias of dissolved oxygen measurements by profiling floats, Umi no kenkyu, 15(6), 479–498.

Kumar, S. P., M. Nuncio, J. Narvekar, A. Kumar, S. Sardesai, S. N. de Souza, M. Gauns, N. Ramaiah, and M. Madhupratap (2004), Are eddies nature's trigger to enhance biological productivity in the Bay of Bengal?, *Geophys. Res. Lett.*, 31, L07309, doi:10.1029/2003GL019274.

Kumar, S. P., P. M. Muraleedharan, T. G. Prasad, M. Gauns, N. Ramaiah,S. N. de Souza, S. Sardesai, and M. Madhupratap, (2002), Why is the Bay of Bengal less productive during summer monsoon compared to the Arabian Sea? *Geophys. Res. Lett.*, 29(24), 2235, doi:10.1029/2002GL016013,

Lévy,M., D. Shankar, J. M. André, S. S. C. Shenoi, F. Durand, C. de Boyer Montégut (2007), Basin-wide seasonal evolution of the Indian Ocean's phytoplankton blooms, *J. Geophys. Res., Oceans*, 112, C12014, doi:10.1029/2007JC004090

Lewis M. R., J. J. Cullen, and T. Platt (1983), Phytoplankton and thermal structure in the upper ocean: consequences of non uniformity in chlorophyll profile, *J. Geophys. Res., Oceans*, 88, C4, 2565–2570.

Li. Z., W. Yu, T. Li, VSN, Murty, and F. Tangang (2013), Bimodal character of cyclone climatology in Bay of Bengal modulated by monsoon seasonal cycle, *J. Clim.*, 26,3, doi:10.1175/JCLI-D-11-00627.1.

Lim. J. Y., Md. L. R. Sarker, L. Zhan, E. Siswanto, A. Mubin, S. Sabarudin (2013), Monitoring long-term ocean health using remote sensing: A case study of the Bay of Bengal.Proc. SPIE 8888, Remote Sensing of the Ocean, Sea Ice, Coastal Waters, and Large Water Regions, 88880K (October 16, 2013). doi:10.1117/12.2029032.

Lin, I.-I. (2012), Typhoon-induced phytoplankton blooms and primary productivity increase in the western North Pacific subtropical ocean, *J. Geophys. Res.*,117, C03039, **d**oi:10.1029/2011JC007626.

Lin, J., D. Tang, W. Alpers, and S. Wang (2014), Response of dissolved oxygen and related marine ecological parameters to a tropical cyclone in the South China Sea, *Advance in space research*, 53,7, http://dx.doi.org/10.1016/j.asr.2014.01.005.

Lukas, R., and E. Lindstrom (1991), The mixed layer of the western equatorial Pacific Ocean, *J. Geophys. Res.*, 96, 3343– 3357.

Madhu, N. V., R. Jyothibabu, P. A. Maheswaran, V. John Gerson, T. C. Gopalakrishnan, and K. K. C. Nair (2006), Lack of seasonality in phytoplankton standing stock (chlorophyll a) and production in the western Bay of Bengal, *Cont. Shelf Res.*, 26, 1868–1883, http://dx.doi.org/10.1016/j.csr.2006.06.004.

Madhupratap, M., M. Gauns, N. Ramaiah, S. Prasanna Kumar, P. M. Muraleedharan, S. N. de Souza, S. Sardesai, and U. Muraleedharan (2003), Biogeochemistry of the Bay of Bengal: Physical, chemical and primary Productivity characteristics of the central and western Bay of Bengal during summer monsoon, *Deep-Sea Res. II*, 50, 5, doi: 10.1016/S0967-0645(02)00611-2.

Mahadevan, A., G. Spiro Jaeger, M. Freilich, M. Omand, E. L. Shroyer, and D. Sengupta (2016), Freshwater in the Bay of Bengal: Its fate and role in air-sea heat exchange, *Oceanography*. 29(2),72–81. http://dx.doi.org/10.5670/oceanog.2016.40.

Mahakur, M., A. Prabhu, A. Sharma, V. Rao, S. Senroy, R. Singh, B. Goswami (2013), A high-resolution outgoing longwave radiation dataset from kalpana-1 satellite during 2004-2012, *Curr. Sci*., 105, 8, 1124-1133.

Maneesha, K., V. P. Sarma, Reddy, Y. Sadhuram, T. V. R. Murty, V. V. Sarma, and M. D. Kumar (2011), Meso-scale atmosphere events promote phytoplankton blooms in the coastal Bay of Bengal, *J. Earth Syst. Sci.*, 120 (4), 773–782,doi:10.1007/s12040-011-0089-y.

Maritorena, S., O. H. F. d'Andon, A. Mangin, D. A. Siegel (2010), Merged satellite ocean color data products using a bio-optical model: Characteristics, benefits and issues. *Remote Sens. Environ.*, 114(8), 1791-1804, doi:10.1016/j.rse.2010.04.002.

Martin, M. V., and C. Shaji (2015), On the eastward shift of winter surface chlorophyll-a bloom peak in the Bay of Bengal. *J. Geophys. Res. Oceans*, 120, 2193–2211, doi:10.1002/2014JC010162.

Martinez-Vicente, V., G. Dall'Olmo, G. Tarran, E. Boss, and S. Sathyendranath, (2013), Optical backscattering is correlated with phytoplankton carbon across the Atlantic Ocean.Geophysical Research Letters, 40, 1–5, doi:10.1002/grl.50252.

McCreary, J. P., Z. Yu, R. Hood, P. N. Vinaychandran, R. Furue, A. Ishida, and K. Richards (2013), Dynamics of the Indian-Ocean oxygen minimum zones, *Progr. Oceanogr.*, 112-113, doi: 10.1016/j.pocean.2013.03.002.

McPhaden, M. J., and G. R. Foltz (2013), Intraseasonal variations in the surface layer heat balance of the central equatorial Indian Ocean: The importance of zonal advection and vertical mixing, *Geophys. Res. Lett.*,40,2737–2741, doi:10.1002/grl.50536

Morel, A, and J-F.Berthon (1989), Surface pigments, algal biomass profiles, and potential production of the euphotic layer: Relationships reinvestigated in view of remote-sensing applications, *Limnol. Oceanogr.*,34, 1545-1562.

Murtugudde, R., S. Signorini, J. Christian, A. Busalacchi, C. McClain, and J. Picaut (1999), Ocean color variability of the tropical Indo-Pacific basin observed by SeaWiFS during 1997-98.*J. Geophys. Res., Oceans,*104, C8, 18351–18366, doi: 10.1029/1999JC900135.

Naik, H., S. W. A. Naqvi, T. Suresh, P. V. Narvekar (2008), Impact of a tropical cyclone on biogeochemistry of the central Arabian Sea, *Global Biogeochem. Cycles*, 22, GB3020, doi:10.1029/2007GB003028.

Najjar, R. G., and R. F. Keeling (1997), Analysis of the mean annual cycle of the dissolved oxygen anomaly in the World Ocean, J. Mar. Res., 55, 117–151.

Narvekar, J., and S. P. Kumar (2006), Seasonal variability of the mixed layer in the central Bay of Bengal and associated changes in nutrients and chlorophyll, *Deep Sea Res. Part I*, 53, 820–835, http://dx.doi.org/10.1016/j.dsr.2006.01.012.

Narvekar, J., and S. P. Kumar (2014), Mixed layer variability and chlorophyll a biomass in the Bay of Bengal, *Biogeosciences*, 11, 3819–3843, doi.10.5194/bg-11-3819-2014.

Pan, J. and Y. Sun, (2013): Estimate of Ocean Mixed Layer Deepening after a Typhoon Passage over the South China Sea by Using Satellite Data. *J. Phys. Oceanogr.*, **43**,498–506, https://doi.org/10.1175/JPO-D-12-01.1

Parampil, S. R., A. Gera, M. Ravichandran, and D. Sengupta (2010), Intraseasonal response of mixed layer temperature and salinity in the Bay of Bengal to heat and freshwater flux, *J. Geophys. Res., Oceans*, 115, C05002, doi:10.1029/2009JC005790.

Park, J. J., Y.-O. Kwon, and J. F. Price (2011), Argo array observation of ocean heat content changes induced bytropical cyclones in the north Pacific, J. Geophys. Res.,116, C12025, oi:10.1029/2011JC007165.

Piontkovski S. A., H. S. Al-Oufi (2014), Oxygen Minimum Zone and Fish Landings along the Omani Shelf, *J. Fish. Aquat. Sci.*, 9: 294-310, doi: 10.3923/jfas.2014.294.310.

Prasad, T.G., (1997), Annual and seasonal mean buoyancy fluxes for the tropical Indian Ocean, *Curr.Sci.*, 73, 667-674, 1997.

Praveen Kumar, B., J. Vialard, M. Lengaigne, V. S. N. Murty, M. J. McPhaden (2011), TropFlux: Air-sea fluxes for the global tropical oceans- description and evaluations, *Climate Dynam.*, 38: 1521, doi: 10.1007/s00382-011-1115-0.

Price, JF., (1981), Upper-ocean response to a hurricane. *J Phys. Oceanogr.*, 11:153–175.

Prince, E. D., and C. P. Goodyear (2006), Hypoxia-based habitat compression of tropical pelagic fishes, *Fish.Oceanogr.*, 15, 451–464, doi:10.1111/j.1365-2419.2005.00393.x.

Rao, K. H., A. Smitha, and M. M. Ali (2006), A study on cyclone induced productivity in southwestern Bay of Bengal during November–December 2000 using MODIS (SST and chlorophyll-*a*) and altimeter sea surface height observations, *Indian J. Mar. Sci.*, 35(2), 153–160.

Rao, R. R., and R. Sivakumar (2000), Seasonal variability of near-surface thermal structure and heat budget of the mixed layer of the tropical Indian Ocean from a new global ocean temperature climatology, *J. Geophys. Res., Oceans*, 105(C1), 995–1015, doi:10.1029/1999JC900220.

Rao, R. R., and R. Sivakumar (2003), Seasonal variability of sea surface salinity and salt budget of the mixed layer of the north Indian Ocean, *J. Geophys.Res., Oceans*, 108, C110.1029/2001JC000907.

Ravichandran, M., M. S. Girishkumar, S. Riser (2012), Observed variability of chlorophyll-a using Argo profiling floats in the southeastern Arabian Sea, *Deep Sea Res. Part I*, 65, 15–25, doi: 10.1016/j.dsr.2012.03.003.

Reddy, P. R. C., P. S. Salvekar, and S. Nayak (2008), Super Cyclone Induces a Mesoscale Phytoplankton Bloom in the Bay of Bengal, *IEEE Geosci. Remote Sens. Lett.*, 5(4), 588-592, doi: 10.1109/LGRS.2008.2000650.

Riser, S. C., and K. S. Johnson (2008), Net production of oxygen in the subtropical ocean, Nature, 451(7176), 323–325, doi:10.1038/nature06441.

Sanford, T.B., J.F. Price, and J.B. Girton, (2011), Upper-Ocean Response to Hurricane Frances (2004) Observed by Profiling EM-APEX Floats. J. Phys. Oceanogr., 41, 1041–1056, https://doi.org/10.1175/2010JPO4313.1doi:10.1002/2016JC01206

Sarma, V.V.S.S., M. S. Krishna, R. Viswanadham, G. D. Rao, V. D. Rao, B. Sridevi, B. S. K. Kumar, V. R. Prasad, Ch. V. Subbaiah, T. Acharyya, D. Bandopadhyay (2013), intensified oxygen minimum zone on the western shelf of Bay of Bengal during summer monsoon: Influence of river discharge, *J. Oceanogr.*, 69(1), 45-55, DOI: 10.1007/s10872-012-0156-2.

Shang, S., L. Li, and F. Q. Sun (2008) Changes of temperature and bio-optical properties in the South China Sea in response to Typhoon Lingling, 2001, Geophysical Research Letters, vol. 35, no. 10, L10602

Shetye, S. R., A. D. Gouveia, D. Shankar, S. S. C. Shenoi, P. N. Vinayachandran, D. Sundar, G. S. Michael, and G. Nampoothiri (1996), Hydrography and circulation in the western BoB during the northeast monsoon, *J. Geophys. Res.*, 101(C6), 14011 – 14026.

Shulenberger, E., Reid, J.L., (1981). The Pacific shallow oxygen maximum, deep chlorophyll maximum, and primary productivity, reconsidered. *Deep-Sea Res.* 28, 901–919.

Smitha, A., K. H. Rao, and D. Sengupta (2006), Effect of May 2003 tropical cyclone on physical and biological processes in the Bay of Bengal, *Int. J. Remote Sens.*, 27, 5301 – 5314, doi:10.1080/ 01431160600835838.

Son, S., T. Platt, C. Fuentes-Yaco, H. Bouman, E. Devred, Y. Wu, and S. Sathyerdranath (2007), Possible biogeochemical response to the passage of Hurricane Fabian observed by satellites, *J. Plankton Res.*, 29, 8, 687-697, doi:10.1093/plankt/fbm050.

Stramma, L., E. D. Prince, S. Schmidtko, J. Luo, and J. P. Hoolihan et al., (2012), Expansion of oxygen minimum zones may reduce available habitat for tropical pelagic fishes, *Nat. Clim. Change.*, 2, 33-37.doi:10.1038/nclimate1304.

Strickland, J.D.H and Parson, T.R. (1965): A Manual of Seawater Analysis. *Bulletin of Fishery Research Board, Canada*, No.125, 2nd Ed., 203pp.

Sudre, J. C Maes, and V Garçon (2013), On the global estimates of geostrophic and Ekman surface currents, *Limnol. Oceanogr.* Methods, 3, 1–20,doi:10.1215/21573689-2071927.

Sun, L, Y.-J.Yang, T. Xian, Z.-M.Lu, and Y.-F. Fu, (2010) Strong enhancement of chlorophyll a concentration by a weak typhoon, Marine Ecology Progress Series, vol. 404, pp. 39–50, 2010.

Takeshita, Y., T. R. Martz, K. S. Johnson, J. N. Plant, D. Gilbert, S. C. Riser, C. Neill, and B. Tilbrook (2013), A climatology-based quality control procedure for profiling float oxygen data, J. Geophys. Res. Oceans, 118, 5640–5650, doi:10.1002/jgrc.20399.

Thadathil, P., I. Suresh, S. Gautham, S. Prasanna Kumar, M. Lengaigne, R. R. Rao, S. Neetu, and A. Hegde (2016), Surface layer temperature inversion in the Bay of Bengal: Main characteristics and related mechanisms, *J. Geophys. Res. Oceans*, 121, 5682–5696, doi:10.1002/2016JC011674.

Thadathil, P., P. M. Muraleedharan, R. R. Rao, Y. K. Somayajulu, G. V. Reddy, and C. Revichandran (2007), Observed seasonal variability of barrier layer in the BoB, *J. Geophys. Res., Oceans* 112, C02009, doi:10.1029/2006JC003651.

Thangaprakash, V. P., M. S. Girishkumar, K. Suprit, N. Suresh Kumar, D. Chaudhuri, K. Dinesh, A. Kumar, S. Shivaprasad, M. Ravichandran, J. T. Farrar, R. Sundar, and R. A. Weller (2016), What controls seasonal evolution of sea surface temperature in the Bay of Bengal? Mixed layer heat budget analysis using moored buoy observations along 90°E, *Oceanography*, 29, 2, 202–213, http://dx.doi.org/10.5670/oceanog.2016.52.

Tummala, S. K., R. S. Mupparthy, M. N. Kumar, S. R. Nayak (2009), Phytoplankton bloom due to cyclone sidr in the central bay of Bengal, *J. Appl. Remote Sens.*, 3(1), 033547. http://dx.doi.org/10.1117/1.3238329.

Udaya Bhaskar, T. V. S., E. Pattabhi Rama Rao, R. VenkatShesu, and R. Devender (2012), A note on three way quality control of Argo temperature and salinity profiles—A semi-automated approach at INCOIS, *Int. J. Earth Sci. Eng.*, 5(6), 1510–1514.

Vaquer-Sunyer, R., and C. M. Duarte (2008), Thresholds of hypoxia for marine biodiversity, *Proceedings of the National Academy of Sciences*, 105 (40), 15452-15457.

Varkey, M. J., V. S. N. Murty, and A. Suryanarayana (1996), Physical oceanography of the BoB and Andaman Sea, *Oceanogr. Mar. Biol*., An Annual Review, 34, 1-70.

Vinayachandran, P. N., Jr. J. P. McCreary, R. R. Hood, K. E. Kohler (2005), A numerical investigation of the phytoplankton bloom in the Bay of Bengal during Northeast Monsoon, *J. Geophys. Res.*, 110, C12001, doi: 10.1029/2005JC002966.

Vinayachandran, P. N., P. Chauhan, M. Mohan, and S. Nayak (2004), Biological response of the sea around Sri Lanka to summer monsoon, *Geophys. Res. Lett.*, 31, L01302, doi:10.1029/2003GL018533.

Vinayachandran, P. N., S. Mathew (2003), Phytoplankton bloom in the Bay of Bengal during the northeast monsoon and its intensification by cyclones, *Geophys. Res. Lett.*, 30, 11, 1572, doi: 10.1029/2002GL016717.

Vinayachandran, P. N., V. S. N. Murty, and V. Ramesh Babu (2002), Observations of barrier layer formation in the BoB during summer monsoon, *J. Geophys. Res.*, 107(C12), 8018, doi:10.1029/2001JC000831.

Vinayachandran, P.N., (2009), Impact of Physical Process on Chlorophyll Distribution in the Bay of Bengal, *Indian Ocean Biogeochemical Processes and Ecological*

Variability Geophysical, Monograph Series, 185, 71-84, doi:10.1029/2008GM000705.

Vincent, E. M., M. Lengaigne, G. Madec, J. Vialard, G. Samson, N. Jourdain, C. E. Menkes, and S. Jullien (2012a), Processes setting the characteristics of sea surface cooling induced by Tropical Cyclones, *J. Geophys. Res*., 117, C02020.doi:10.1029/2011JC007396

Vincent, E. M., M. Lengaigne, J. Vialard, G. Madec, N. Jourdain, and S. Masson (2012b) Assessing the oceanic control on the amplitude of sea surface cooling induced by Tropical Cyclones, *J. Geophys. Res.,* 117: doi: 10.1029/2011JC007705.

Virginie Thierry, B. Henry (2016), The Argo quality control manual for dissolved oxygen concentration. The Argo-BGC Team, doi: 10.13155/46542.

Wong, A., R. Keeley, T. Carval (2015), Argo quality control manual for CTD and trajectory data, the Argo Data Management Team, doi:10.13155/33951.

Wyrtki, K. (1971) Oceanographic Atlas of the International Indian Ocean Expedition. National Science Foundation, Washington, DC. 53.

Xing, X., H. Claustre, J. Uitz, A. Mignot, A. Poteau, and H. Wang (2014), Seasonal variations of bio-optical properties and their interrelationshipsobserved by BGC-Argo floats in the subpolar North Atlantic, J. Geophys. Res. Oceans, 119, doi:10.1002/ 2014JC010189.

Yu, J., D. L. Tang, Y. Z. Li, Z. Huang, G. B. Chen (2013), Increase in fish abundance during two typhoons in the South China Sea, *Adv. Space Res.*, 51 (2013), 1734–1749.

Zhang, H., D. Chen, L. Zhou, X. Liu,T. Ding, and B. Zhou (2016), Upperocean response to typhoon Kalmaegi(2014),J. Geophys. Res. Oceans,121,6520–6535.

Jaimes, B., Shay, L. K., and Halliwell, G. R. (2011).The response of quasigeostrophic oceanic vortices to tropical cyclone forcing. Journal of Physical Oceanography, 41, 1965–1985.

Table-1. Observations from daily ASCAT data and 3 hourly best track data when TC was nearest to the C-Float location.

Parameters	TC *Hudhud*	TC *Vardah*
Satellite wind speed (m s^{-1}) averaged over the box near to the C-Float	15	17
Maximum Sustained Surface Wind (kt) from best track data	55	60
24 hour average of maximum Sustained Surface Wind (kt) from best track data	50	60
Average translation speed (km/hr) of TC 12 hour before and after TC	11	18.5

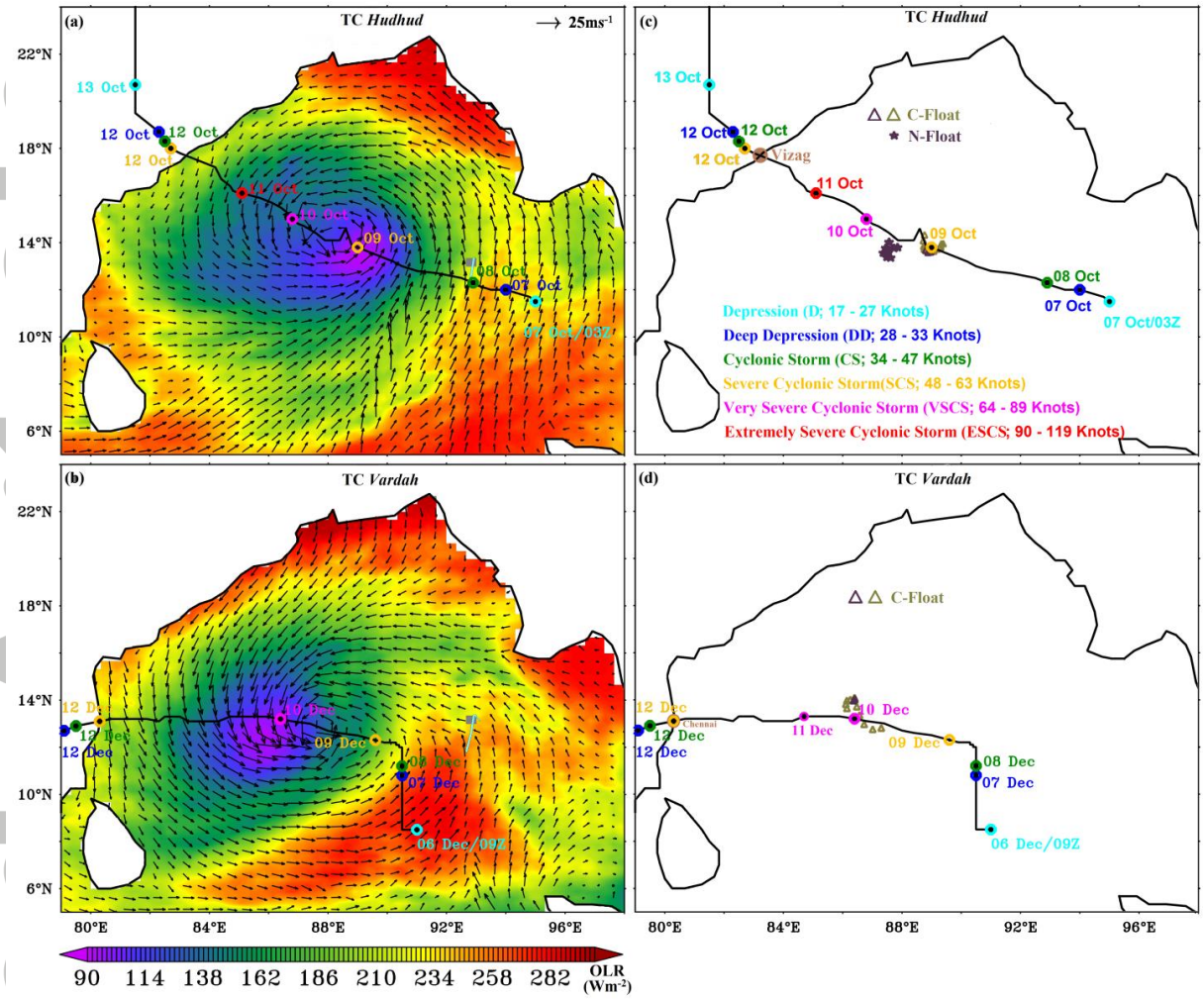

Figure 1. ASCAT wind speed vectors (m s^{-1}) and OLR (Wm^{-2}) on 9 October, 2014 during TC *Hudhud* (panel a) and on 10 December, 2016 during TC *Vardah* (panel b) when TC's were nearer to the C-Float profiling locations. The six hourly best track (black line) and intensity (open coloured circles corresponding to the dates and intensity) of TC *Hudhud* (panel a and c) *and* TC *Vardah* (panel b and d) obtained from Regional Specialised Meteorological Centre (RSMC), IMD, India (http://www.imd.gov.in/section/nhac/dynamic/bestrack.htm) are marked. The classification of tropical systems by IMD with respect to wind speed are classified as: Depression (D) (17–27 knot; kt), Deep Depression (DD) (28–33 kt), Cyclonic Storm (CS) (34–47 kt), Severe Cyclonic Storm (SCS) (48–63 kt), Very Severe Cyclonic Storm (VSCS) (64–89 kt), and Extremely Severe Cyclonic Storm (ESCS) (90-119 kt) and are marked as cyan, blue, green, orange, purple and red circles respectively along the track of TCs. The number adjacent to each circle indicates dates.Triangles in the right panels (c and d) indicates the C-Float (WMO ID 2902114) with chlorophyll sensor profiling locations during TC *Hudhud* (15 September, 2014 to 15 November, 2014; panel c; dark green triangle) and TC *Vardah* (15 November 2016 to 15 January 2017; panel d; dark green triangle). Dark purple triangle indicates C-Float profiling locations in close proximity during the period of TC *Hudhud*; 7-14 October 2014 (panel c) and TC *Vardah*; 6–12 December 2016 (panel d). The dark purple star in panel (c) indicates N-Float (WMO ID 5903712) with nitrate sensor profiling locations during September-December 2014.

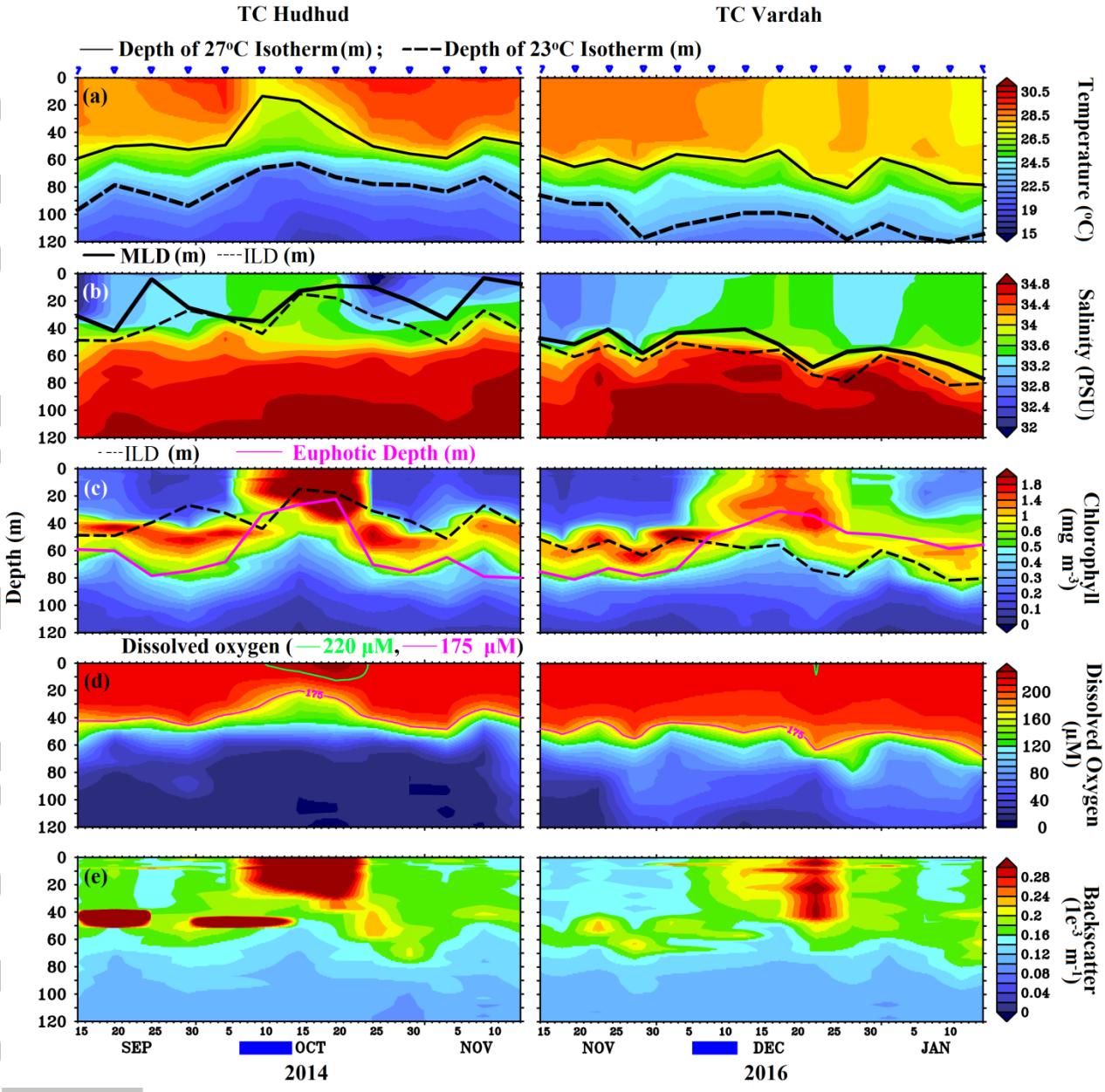

Figure 2. Temporal evolution of depth-time section of (a) temperature (°C), (b) salinity, (c) Chlorophyll (mg m^{-3}), (d) Dissolved Oxygen (µM) and (e) optical backscatter (1e-3 m^{-1}) from C-Float (WMO ID 2902114) during 15 September, 2014 to 15 November, 2014 (left panels; TC *Hudhud*) and 15 November 2016 to 15 January 2017 (right panels; TC *Vardah*) in the south-western BoB. In panel (a), thick dashed line: depth of 23°C isotherm (m) and thin black line: depth of 27°C isotherm. In panel (b), thick black line: MLD (m), and thin black dash line: ILD (m). In panel (c), thick pink line: euphotic depth, and thin black dash line: ILD (m). In panel (d), thin pink (green) line: depth of 175 (220) µM dissolved oxygen (m). Blue thick line in the bottom of the figure indicates TC *Hudhud* period (7–14 October, 2014; left panel) and TC *Vardah* (6-12 December, 2016). The blue inverted triangle on top of the panel (a) indicates the surfaced date of C-Float profiling measurements.

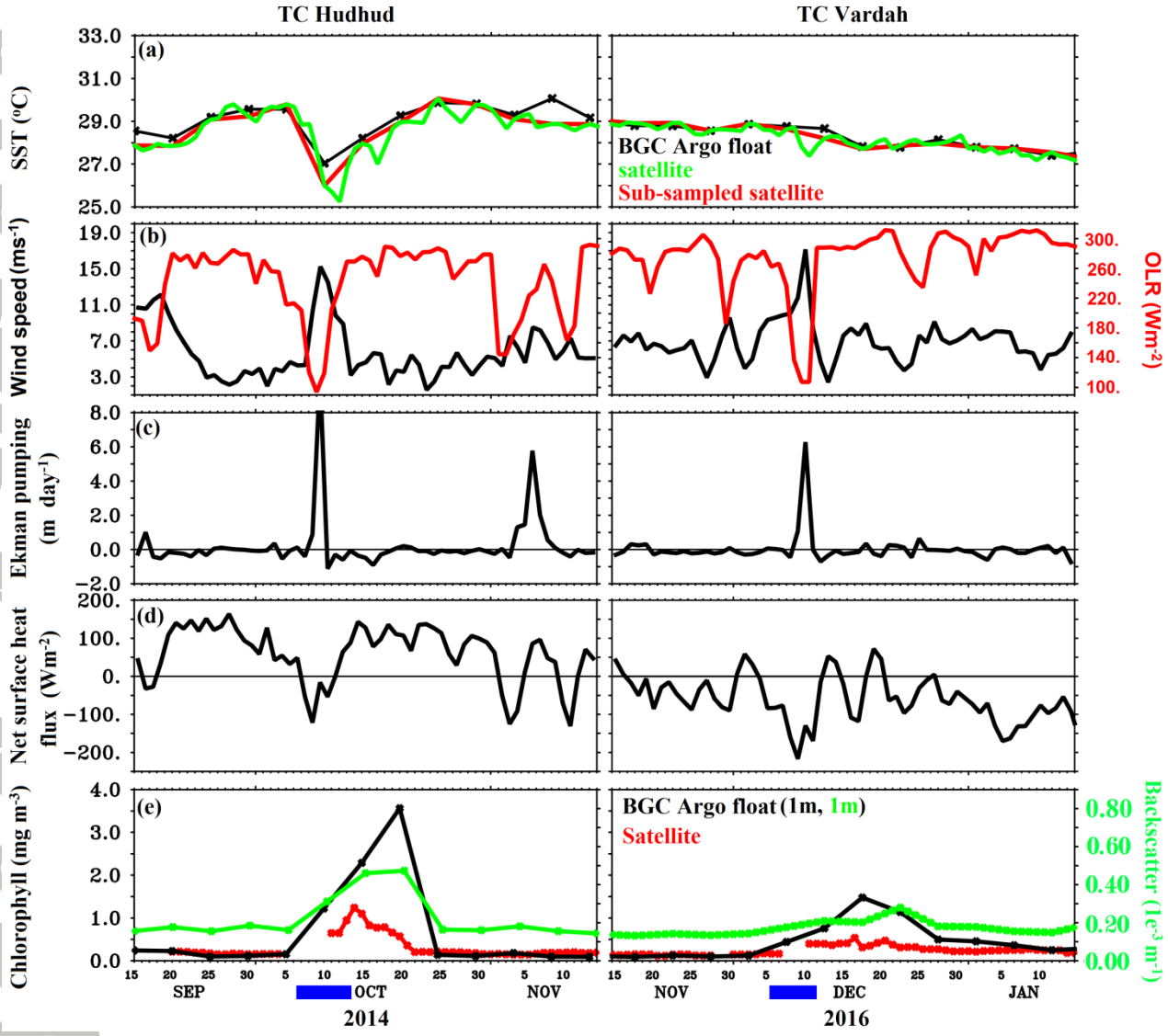

Figure 3. Temporal evolution of (a) C-Float 1 m temperature (black line, °C), MW-OI SST (green line, °C) and MW-OI SST sub-sampled to biogeochemical C-Float temporal resolution (5-day; similar to black line) (red line °C), (b) wind speed (black line, m s^{-1}) and OLR (red line; Wm^{-2}), (c) Ekman pumping velocity (m day^{-1}), (d) Net surface heat flux (W m^{-2}) and (e) C-Float Chlorophyll (black line, mg m^{-3}) and optical backscatter (green line; m^{-1}) at 1 m and satellite merged daily chlorophyll (red line, mg m^{-3}) during 15 September 2014 to 15 November 2014 (left panel; TC *Hudhud*) and 15 November 2016 to 15 January 2017 (right panel; TC *Vardah*). Except C-Float measurements all the parameter averaged over the box 13.25°N–14°N and 88.45°E–89.25°E for TC *Hudhud* (marked as brown box in Figure 4f) and averaged over the box 13.55°E–14.3°E and 86.2°E–87.0°E for TC *Vardah* (marked as brown box in Figure 4h). Blue thick line in the bottom of the figure indicates TC *Hudhud* period (7–14 October, 2014; left panel) and TC *Vardah* period (6-12 December, 2016).

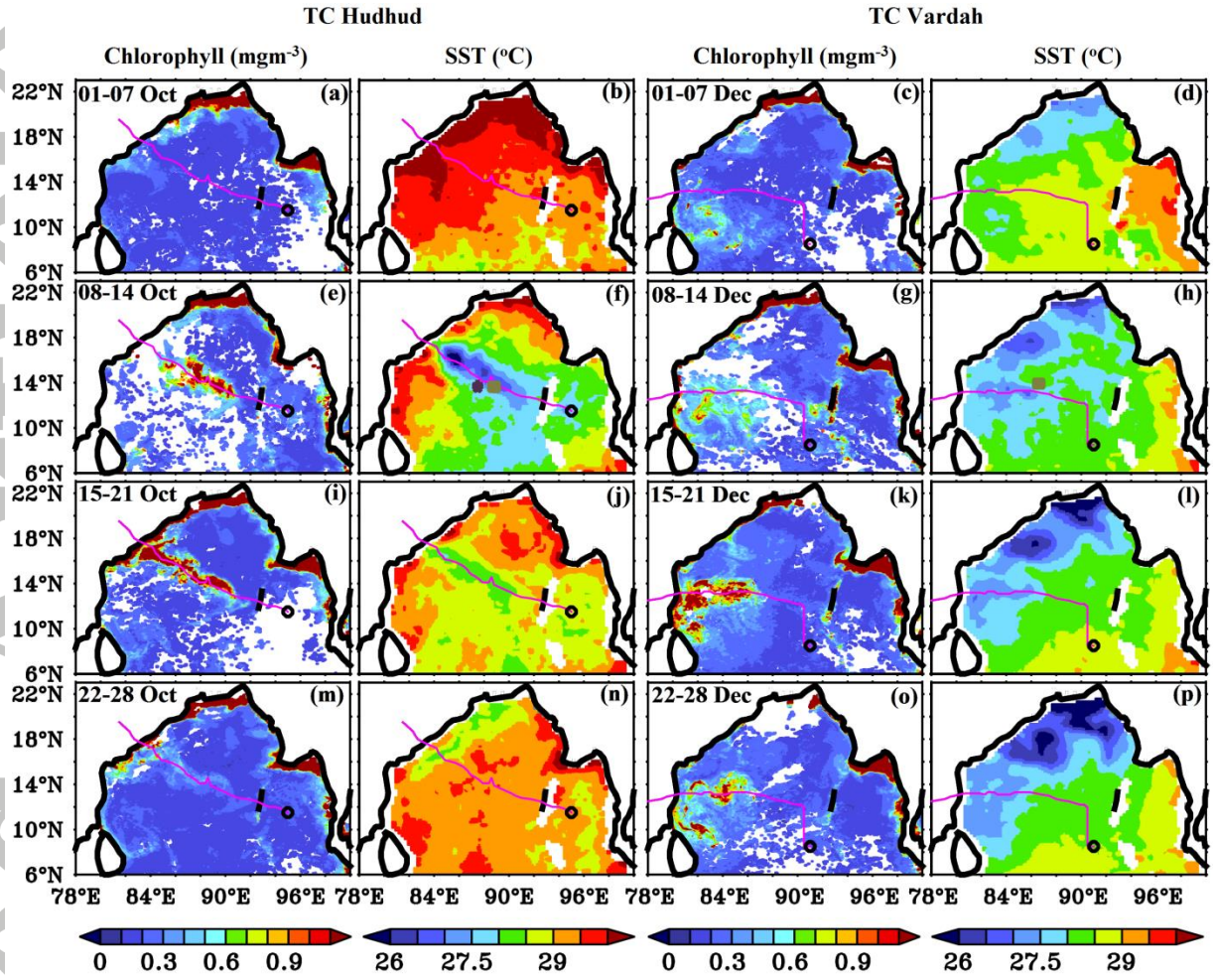

Figure 4. 7-day composites of MODIS chlorophyll-*a* (mg m^{-3}; first and third column) and MW-OI SST (°C; second and fourth column) during TC *Hudhud* ((a and b) 1-7 October, 2014 (e and f) 8-14 October, 2014 (i and j) 15-21 October, 2014 and (m and n) 22-28 October, 2014) and TC *Vardah* ((c and d) 1-7 December, 2016 (g and h) 8-14 December, 2016 (k and l) 15-21 December, 2016 and (o and p) 22-28 December, 2016) period. In the panels the pink line indicates TC tracks and black circle indicates TCs genesis location (TC *Hudhud* first and second column; TC *Vardah*-third and fourth column). In the panel (f) the brown box represents the area (13.25°N-14°N and 88.45°E-89.25°E) for TC *Hudhud* and in the panel (h) brown box represents the area (13.55°E-14.3°E and 86.2°E-87.0°E) for TC *Vardah* when it is close to C-Float location.

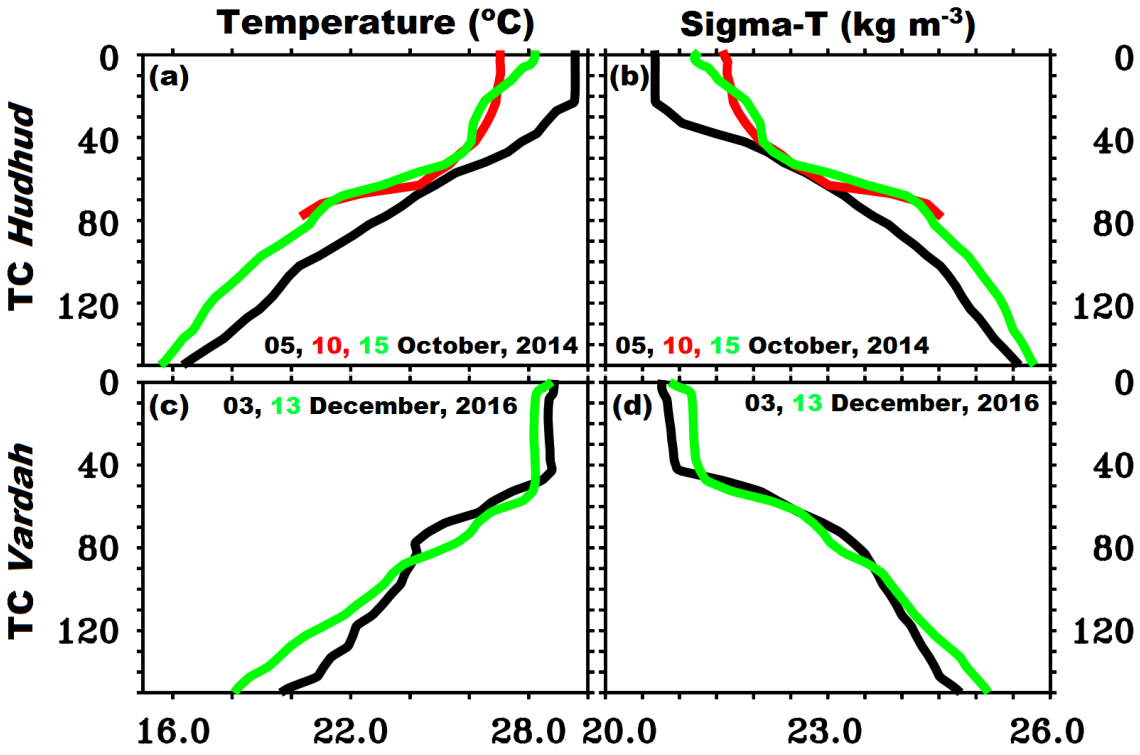

Figure 5. (a and b) Temperature (°C) and (c and d) sigma-t (Kg m^{-3}) profiles from the C-Float before (black), during (red) and after (green) the TC. (a and b) TC *Hudhud* and (c and d) TC *Vardah.*

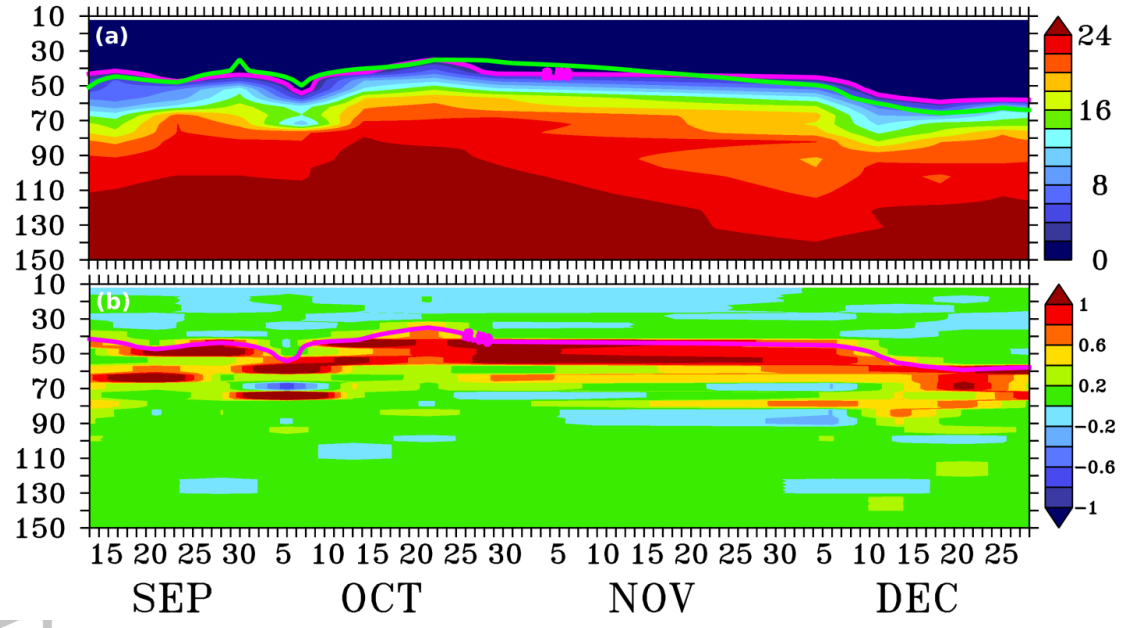

Figure 6. Depth-time section of (a) nitrate (μM) and (b) vertical gradient of nitrate (μM m^{-1}) from the N-Float (WMO ID 5903712; the location of N-Float is marked in figure 1c as purple star) during September-December, 2014. The pink and green line indicates depth of nutricline (defined as 2.5 μM) and ILD (m).

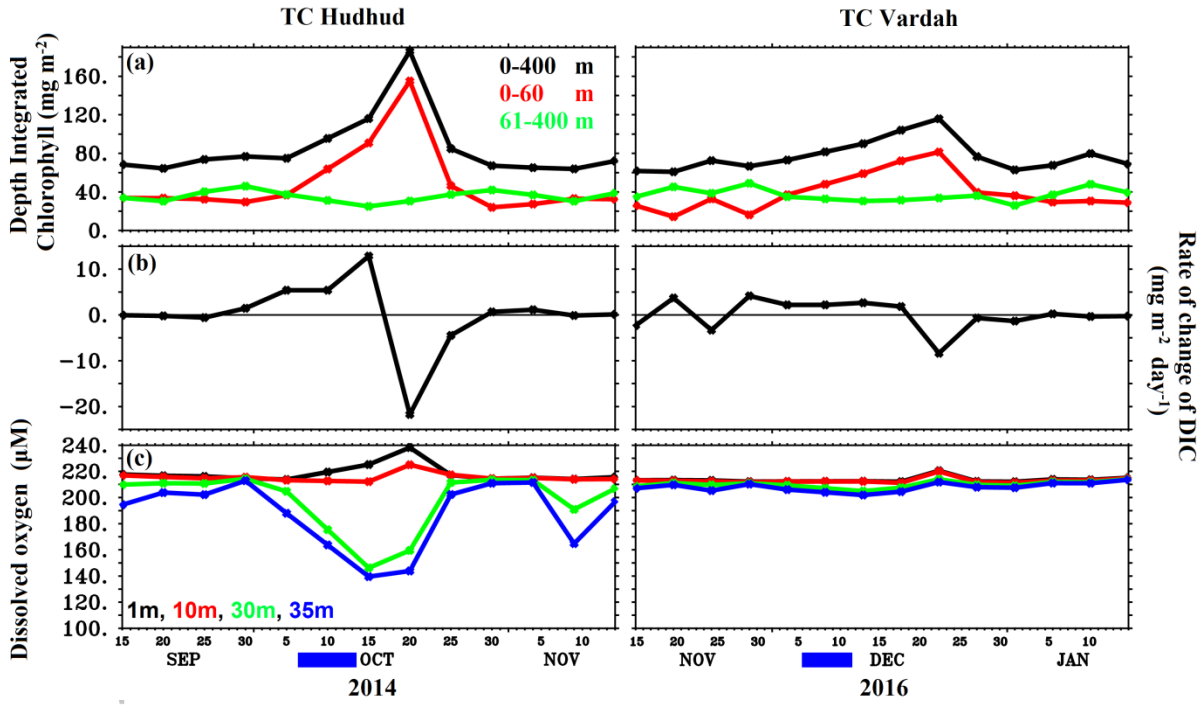

Figure 7. Temporal evolution of (a) depth integrated chlorophyll (mg m^{-2}; 0–60 m red line; 0–400 m black line; 61–400 m green line), (b) rate of change of depth (0–60 m) integrated chlorophyll (mg m^{-2} day^{-1}) and (c) dissolved oxygen (µM) at 1m (black line), 10 m (red line), 30 m (green line) and 35 m (blue line). Blue thick line in the bottom of the figure indicates TC *Hudhud* period (7–14 October, 2014; left panel) and TC *Vardah* (6-12 December, 2016; right panel).

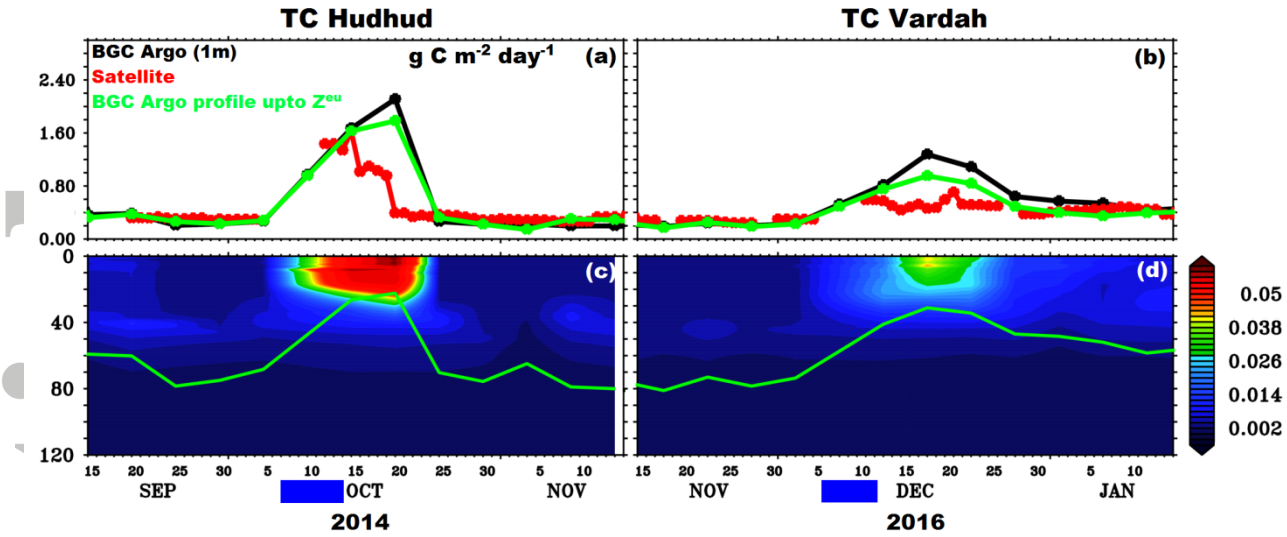

Figure 8. Temporal evolution of integrated primary productivity (PP) from the surface to euphotic depth (g C m^{-2} day^{-1}): using satellite merged chlorophyll-*a* (mg m^{-3}) and MW-OI SST (°C) (PP_{zeu}^{Sat}, redline); using surface chlorophyll-*a* (mg m^{-3}) and surface temperature (°C) from the C-Float and (PP_{zeu}^{Surf} black line); and using chlorophyll and temperature profiles from the C-Float ($PP_{zeu}^{STD-VGPM-P}$; green line) during (a) TC *Hudhud* and (c) TC *Vardah*. Temporal evolution of PP profiles ($PP_{z}^{STD-VGPM-P}$; g C m^{-3} day^{-1}) estimated from the BGC-Argo chlorophyll and temperature profiles during (b) TC *Hudhud* and (d) TC *Vardah*. The green solid line in the panel b and d represents the euphotic depth. Blue thick line at the bottom of the figure indicates TC *Hudhud* period (7–14 October, 2014; left panel) and TC *Vardah* (6-12 December, 2016) period.

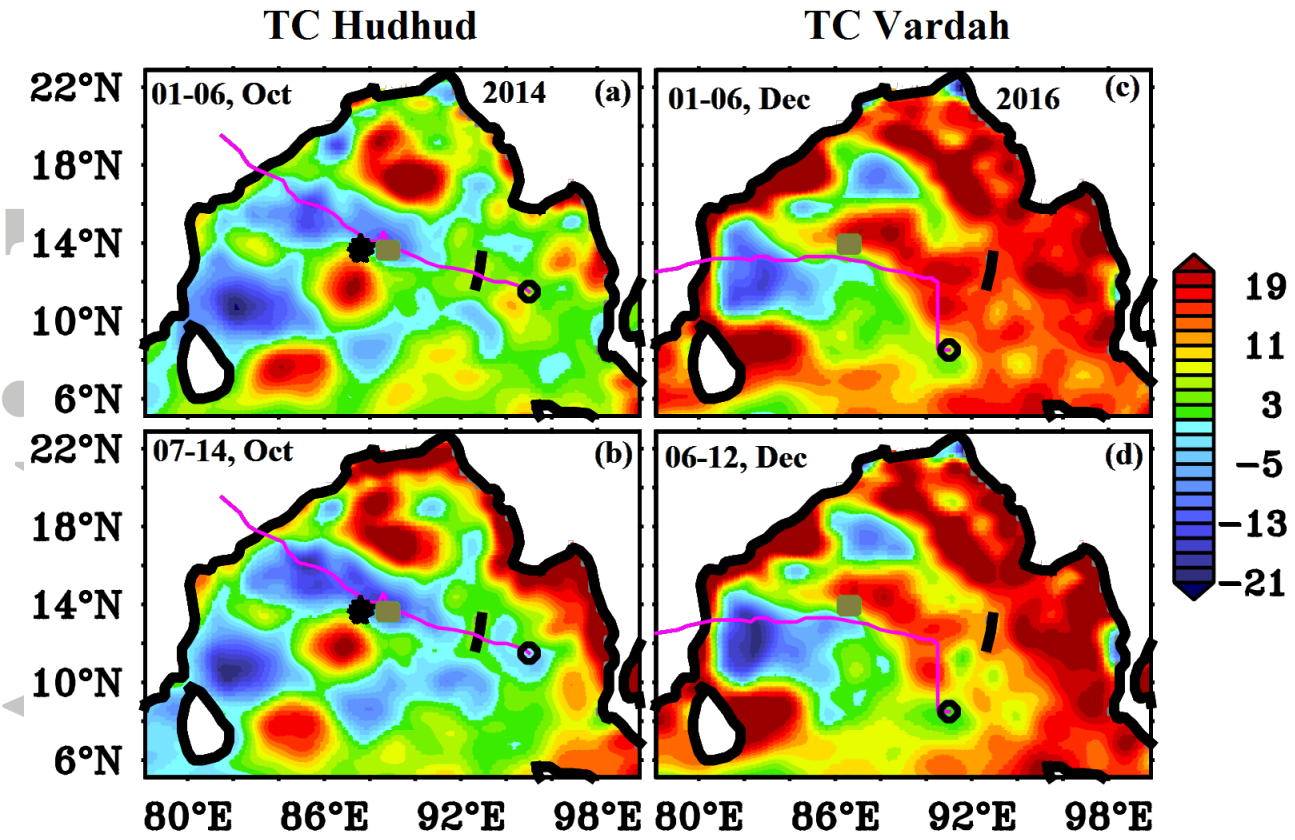

Figure 9. 7-day composite of SSHA (cm) before and after the TCs (left panel-TC *Hudhud* and right panel-TC *Vardah*). In the panels the pink line indicates TC tracks and black circle indicates TCs genesis location. In the left panels the brown box represents the area (13.25°N-14°N and 88.45°E-89.25°E) for TC *Hudhud* and in the right panel brown box represents the area (13.55°E-14.3°E and 86.2°E-87.0°E) of C-Float profiled locations when it was close to TC *Vardah*. Dark purple star indicates locations of N-Float.